ubiquitination by preincubation for 30 min. Taking these results together, we suggest that PCNA interacting with either pol δ or RFC on DNA is a better target of RAD6A–RAD18, rather than PCNA just encircled on DNA.

PCNA mono-ubiquitination can be coupled to DNA replication

Next, we asked whether the PCNA molecules in the replication machinery consisting of pol δ and RFC during elongation reactions[33] are able to be a target. To address this question, we reconstituted the DNA replication reaction with pol δ in the presence of UEs under the ubiquitin assay conditions described in Fig. 1b. DNA synthesis was monitored in the additional presence of [α-^{32}P] dTTP (Fig. 3). The time course was analyzed by alkaline agarose gel electrophoresis of the products (Fig. 3a and b), and incorporation of radioactivity was determined (Fig. 3c). The results demonstrated that UEs exhibited no influence on the size of the product (Fig. 3a and b) and total amounts of DNA synthesis (Fig. 3c). This is consistent with findings in a yeast system.[9]

Then, mono-ubiquitination of PCNA was monitored by Western blotting under the same conditions as shown in Fig. 3b. The results demonstrated that PCNA molecules interacting functionally with pol δ during elongation were able to be ubiquitinated (Fig. 4a and b). In the absence of dCTP, further stimulation by addition of pol δ was not observed (Fig. 4a and b), suggesting the levels of stimulation by each of RFC and pol δ to be equivalent and not additive for the following reasons. In the reaction without pol δ, RFC forms complex with PCNA at apparently all the 3′-ends.[33] Such PCNA molecules interacting with RFC could be ubiquitinated efficiently (Fig. 2f). By addition of pol δ, the same number of PCNA molecules now could make complexes with pol δ at the 3′-ends. Those PCNA molecules interacting with pol δ could be again better targets for ubiquitination (Fig. 2f). In spite of addition of pol δ, the number of PCNA molecules interacting with either RFC or pol δ should be constant. Therefore, it was very surprising that the ubiquitination of PCNA was stimulated by DNA synthesis (Fig. 4a and b), since the number of PCNA molecules interacting with pol δ must be constant during elongation reactions in consideration of the fact that pol δ should interact with PCNA at only the 3′-ends.

To address why the elongation reaction stimulated the ubiquitination, we analyzed the status of PCNA molecules on the DNA by a previously established method to isolate PCNA–DNA complexes in reaction mixtures for DNA replication (Fig. 4c).[33] A primer containing an extended 5′ tail with one biotin molecule was annealed to mp18 ssDNA (Fig. 4c). The 5′ tail of the primer did not exert any influence on DNA synthesis (data not shown).[33] The primed mp18 ssDNA molecules were attached to magnetic beads, and then DNA replication reactions with RFs, UEs, and pol δ were carried out as

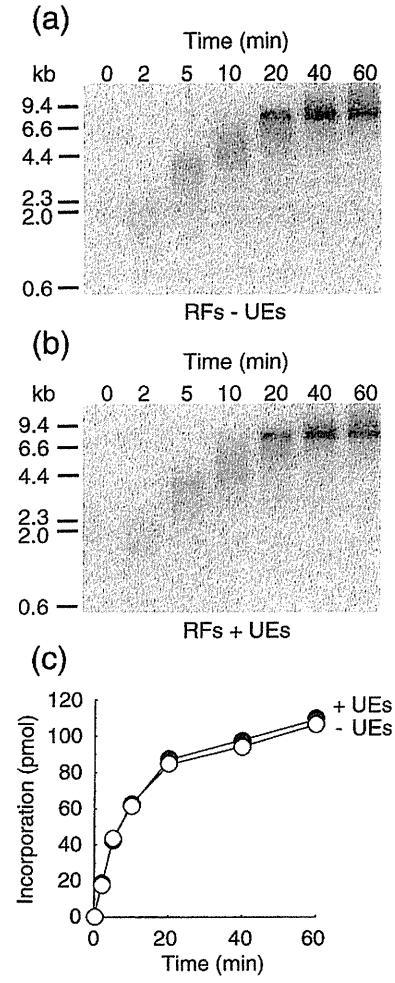

Fig. 3. Pol δ holoenzyme assays in the presence or absence of UEs. (a and b) Time courses of DNA synthesis in the presence (b) or absence (a) of UEs. Reactions were carried out for the indicated times under standard assay conditions with pol δ (380 fmol). Products were analyzed by 0.7% alkaline agarose gel electrophoresis. (c) Incorporation of dNMP was measured as described in Materials and Methods.

described in Fig. 4c. After reactions for 10 min, the beads were washed and bound PCNA was detected by Western blotting (Fig. 4d). Chemiluminescence signals detected with a CCD camera were quantified with reference to a standard curve for PCNA in the same blot (Fig. 4e). We have demonstrated previously that the assay detects PCNA molecules that are loaded on DNA in an RFC-dependent manner.[33]

First, general properties of loaded PCNA in DNA replication in the absence of RAD6A–RAD18 were analyzed (Fig. 4d and e, lanes 1–4).[33] The amount of PCNA detected in reactions with RFC alone was 54 (±7) fmol (Fig. 4d and e, lane 2). Since the background signal, which is the amount of PCNA detected after linearization of DNA with a restriction enzyme, HincII, was 29 (±4) fmol (Fig. 4d and e, lane 4), we estimated that the net amount of loaded PCNA could be about 25 fmol, equivalent to the amount of the primer template (33 fmol) (Fig.

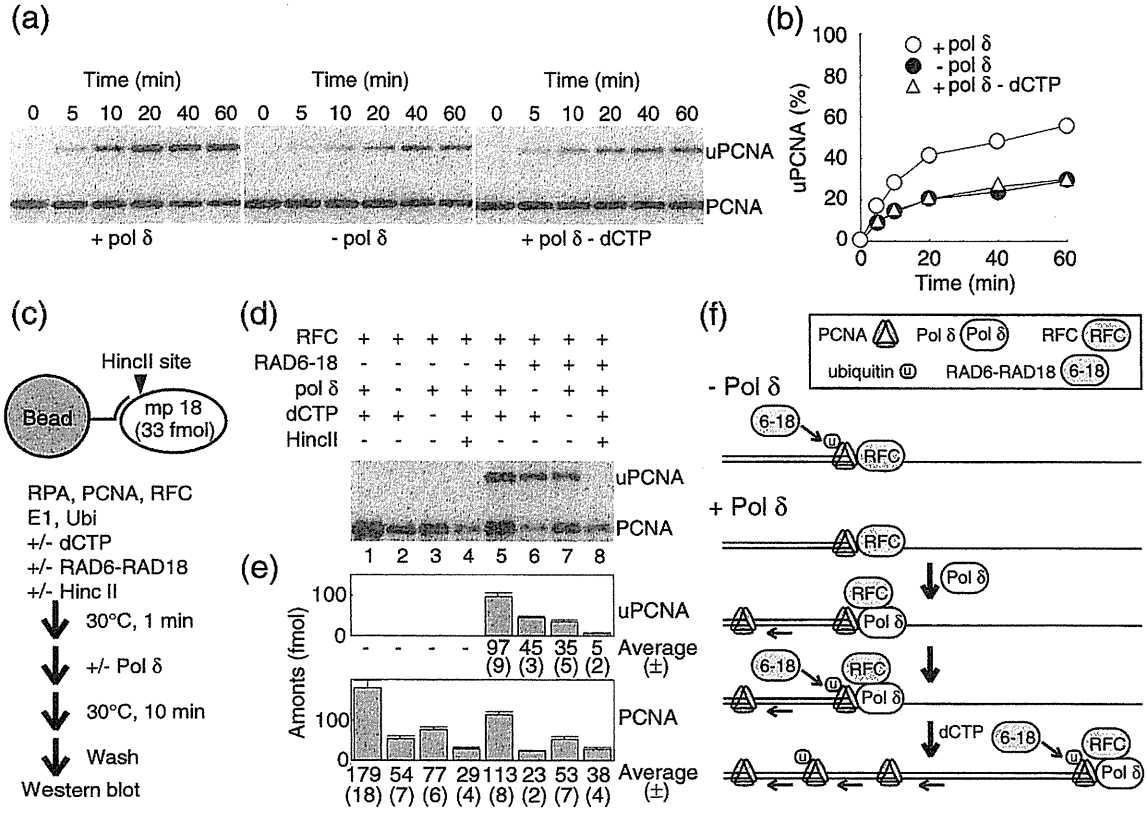

Fig. 4. PCNA mono-ubiquitination coupled with DNA replication. (a and b) Time courses of reactions for PCNA mono-ubiquitination in the presence or absence of pol δ (380 fmol) and/or dCTP. The reactions were carried out under the conditions described in Figs. 1b and 3b and in Materials and Methods. Reaction products were analyzed by Western blotting using anti-PCNA antibodies (a). The signal intensity detected by a CCD camera was quantified, and averages of three to five independent experiments were plotted as the relative amount of the mono-ubiquitinated form (b). Error bars are smaller than their symbols. (c) Outline of the assay to determine amounts of PCNA loaded on DNA. DNA was attached to magnetic beads via biotin–streptavidin linkage. The reactions were carried out for 10 min with the indicated factors in the presence or absence of pol δ (380 fmol). After termination of the reactions, the beads were washed and bound PCNA was analyzed by Western blotting (d and e). (d) A representative image of the Western analysis. uPCNA represents mono-ubiquitinated PCNA. (e) Chemiluminescence signals detected with a CCD camera were quantified with reference to a standard curve for PCNA in the same blot. Averages of four independent experiments with SD in parentheses were shown with graphs. (f) Conceivable protein actions based on the model proposed previously.[33] After loading by RFC, PCNA in the complex was ubiquitinated during 10 min incubation. Addition of pol δ induced dynamic actions so that additional PCNA molecules were loaded on DNA. Probably, the PCNA molecules interacting with pol δ were preferentially ubiquitinated as shown in Fig. 2f. Primer extension by addition of dCTP facilitated further accumulation of PCNA on DNA. PCNA molecules that were released behind the 3′-end before ubiquitination were not better substrates for ubiquitination, resulting in coexistence of ubiquitinated and ubiquitin-free PCNA molecules in a mosaic fashion.

4e, note the difference between lanes 2 and 4) with approximately one PCNA molecule loaded onto template DNA.[33,47,48] Addition of pol δ in the absence of dCTP raised the amount of PCNA slightly (Fig. 4d and e, lane 3). Consequently, approximately 48 fmol of PCNA was detected on the 90-mer primer (Fig. 4e, the difference between lanes 3 and 4) corresponding to one to two molecules on DNA, as illustrated in Fig. 4f.[33] Primer extension by addition of dCTP facilitated further accumulation of PCNA on DNA to about 150 fmol of the net amount of PCNA (Fig. 4e, lane 1, note the difference between lanes 1 and 4) corresponding to four to five molecules on DNA, as illustrated in Fig. 4f.[33,48]

Then, we analyzed ubiquitinated PCNA by introduction of RAD6A–RAD18 into the reaction mixture (Fig. 4d and e, lanes 5–8). In the absence of pol δ, almost all PCNA molecules were detected as ubiquitinated forms (Fig. 4d, lane 6). Introduction of pol δ in the absence of dCTP did not appreciably affect the amount of ubiquitinated PCNA (the slight reduction might be attributed to pull-down efficiencies of the experiment, which could be affected slightly by respective protein factors), even though the total amount was increased (Fig. 4d, lanes 3 and 7). Consequently, the significant fraction of PCNA on DNA persisted without ubiquitination, even in the presence of excess amounts of UEs. Primer extension with dCTP further increased the amount of ubiquitinated PCNA, but significant fractions of PCNA remained without ubiquitination (Fig. 4d, lane 5). These results are consistent with the observation in Fig.

2f, which is that the PCNA molecules, just encircled on DNA, are not efficient targets for ubiquitination, but rather PCNA molecules, proximately located at the 3′-end and making complex with pol δ as illustrated in Fig. 4f. We suggest that stimulation of ubiquitination by DNA synthesis was mainly a consequence of continuous loading of PCNA onto the DNA and subsequent ubiquitination of the newly loaded PCNA molecules.

Reconstitution of DNA replication on a damaged template with polymerase switching between pol δ and pol η

It is critical to ask whether polymerase switching reactions between pol δ and translesion pols are observed in this *in vitro* system. To reconstitute polymerase switching, we used UV-irradiated mp18 ssDNA as a template. First, mp18 ssDNA was irradiated with different doses of UV (50–1600 J/m^2) after which its capacity as a template for replication with pol δ was examined (Supplementary Fig. S4). The result showed DNA synthesis to be inhibited in a UV dose-dependent manner. Under these reactions, ubiquitination of PCNA was similarly reduced and reached a level equivalent to that without dCTP on the template irradiated with the highest dose (1600 J/m^2), at which most of DNA synthesis was blocked just like that without dCTP (Supplementary Fig. S4a–c). By determining the status of PCNA mono-ubiquitination on UV-irradiated DNA by the method as shown in Fig. 4c, we concluded that the reduction of PCNA ubiquitination with UV-irradiated templates could be attributed to the reduced amounts of PCNA on DNA during elongation reactions (Supplementary Fig. S4d and e).

In the following experiments, we chose a template irradiated at 100 J/m^2, with which significant reduction of the full-length products was observed (Supplementary Fig. S4a). Since the lesions inhibited elongation with pol δ (Supplementary Fig. S4a), we could detect further elongation by addition of pol η when polymerase switching occurred.[49,50] After reactions in the presence of increasing amounts of pol η without RAD6A–RAD18, the products were analyzed by alkaline agarose gel electrophoresis (Fig. 5a). The results showed that the average size of the products was increased in a manner dependent on the amount of pol η up to 0.2 pmol (Fig. 5a, lanes 1–8 and graphs). However, further addition of excess pol η resulted in a decreased size of products, suggesting inhibitory effects on elongation (Fig. 5a, lanes 8–11 and graphs). When the template was replaced with intact mp18 DNA, inhibitory effects

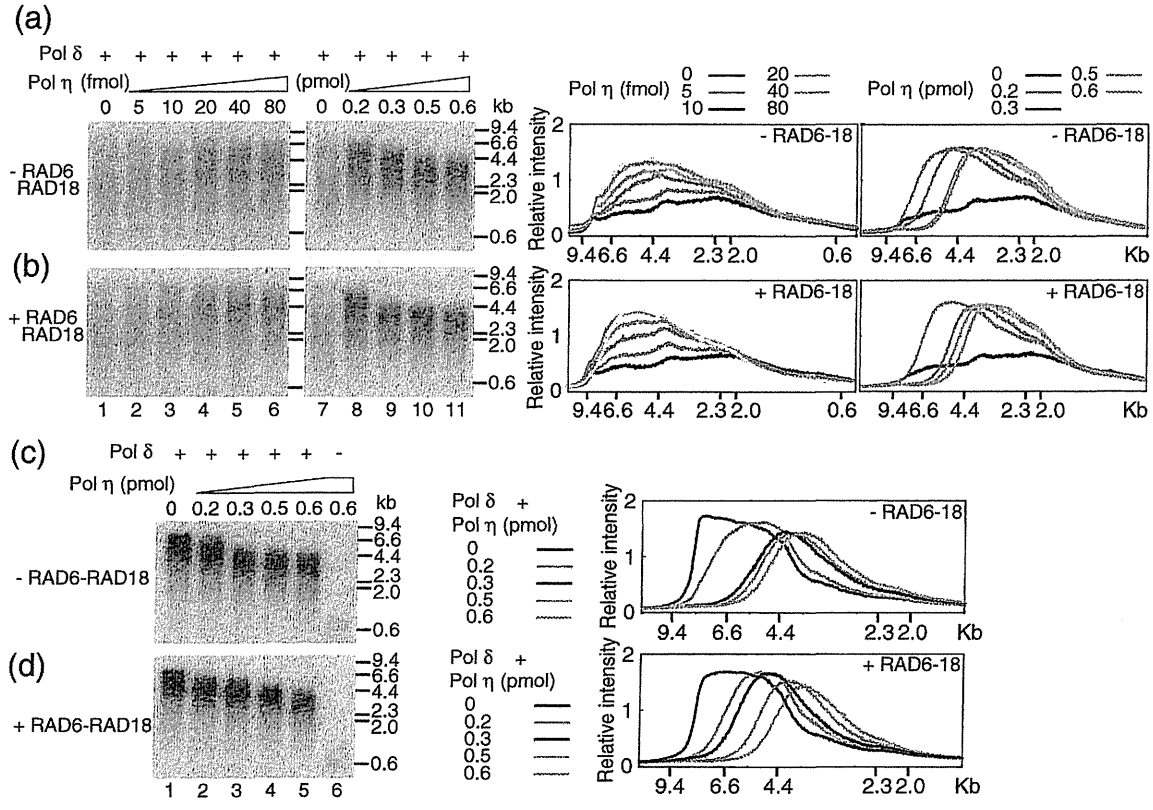

Fig. 5. Reconstitution of PCNA mono-ubiquitination-independent polymerase switching on UV-irradiated templates. Titration of pol η under standard reaction conditions containing RFs and UEs in the presence of pol δ (380 fmol). Intact (c and d) and UV-irradiated mp18 DNA (100 J/m^2) (a and b) were used as templates. Reactions were carried out for 10 min with the indicated amounts of pol η, in the presence (b and d) or absence (a and c) of RAD6A–RAD18. Products were analyzed by 0.7% alkaline agarose gel electrophoresis. The gel images were analyzed by Multi Gauge software (FUJIFILM), and the relative intensity of each lane is shown as a function of the product size in graphs.

on the elongation were also observed (Fig. 5c). By monitoring polymerase activity of pol η itself, we detected products around 0.6 kb with the maximum amount of pol η (Fig. 5c, lane 6), suggesting a much lower capacity for replication than with pol δ. We consider that the inhibition could be due to competitive association of pol η at 3′-ends. Such competition was not detected even when large amounts of pol β were introduced into the reaction mixture (Supplementary Fig. S5). These results indicated that pol η mechanistically has the potential to access 3′-ends without ubiquitination of PCNA and that polymerase switching between pol δ and pol η occurs frequently and spontaneously during DNA synthesis in this *in vitro* system.

Then, RAD6A–RAD18 was introduced to assess the effect of PCNA ubiquitination (Fig. 5b). The result showed that the size of products was also increased by addition of pol η, although we could not detect a clear difference from reactions without RAD6A–RAD18 using a wide range of concentrations of pol η (Fig. 5a and b). Furthermore, stimulation of pol η itself was also not clear (Fig. 5c and d, lane 6), which might be due to resolution of the products in this gel system. We considered the possibility that the concentration of template was sufficiently high for pol η to access 3′-ends without interaction with ubiquitinated PCNA.[51–53] To test this possibility, we reduced the concentration of the template as far as possible (Fig. 6). Again, the control

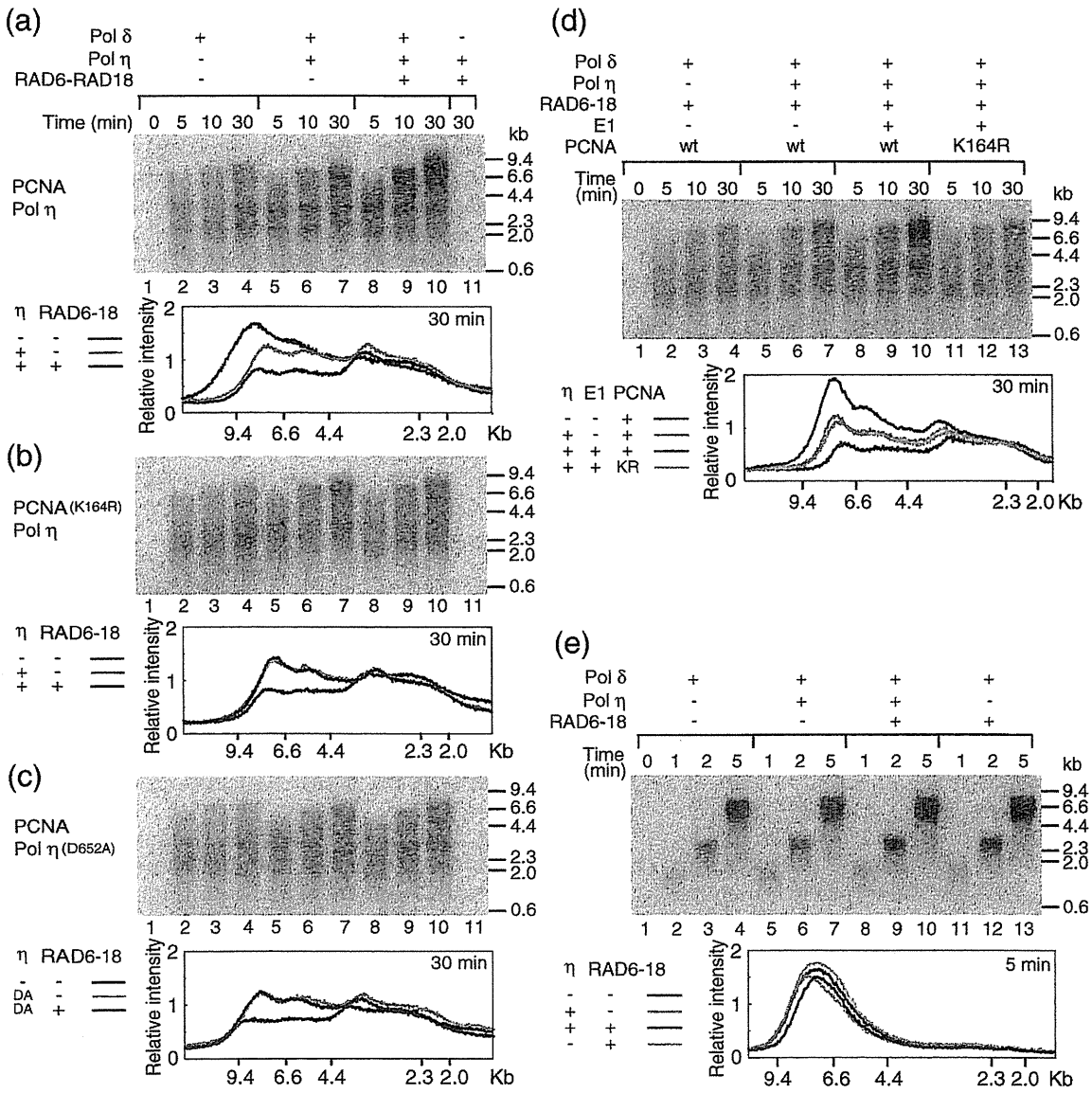

Fig. 6. Reconstitution of PCNA mono-ubiquitination-dependent polymerase switching on UV-irradiated templates. Intact (e) or UV-irradiated mp18 DNAs (100 J/m^2) (a–d) were used as templates. Reactions containing RFs, UEs, and indicated pols were carried out for the indicated times under the conditions described in Materials and Methods. For (b)–(d), wild-type proteins were replaced with the indicated mutants. Products were analyzed by 0.7% alkaline agarose gel electrophoresis. The gel images were analyzed by Multi Gauge software (FUJIFILM), and the relative intensity of each lane at 30 min (for UV-irradiated templates) or 5 min (for intact templates) is shown as a function of the product size in graphs.

reaction with pol δ alone showed a smear size distribution of the products, which was due to stalling of DNA replication (Fig. 6a, lanes 2–4 and graph). When pol η was introduced (Fig. 6a, lanes 5–7 and graph), an increase in the products (around 7 to 4 kb) was observed, demonstrating again ubiquitination-independent polymerase switching. Moreover, we now detected further accumulation of full-length products on addition of RAD6A–RAD18 (Fig. 6a, lanes 8–10 and graph). Under these reaction conditions, pol η seemed to be hardly contributing to gross DNA replication because no products were detectable after 30 min reaction with pol η in the absence of pol δ (Fig. 6a, lane 11). Notably, when the template was replaced with intact DNA, the replication finished after 5 min, and RAD6A–RAD18 and pol η were without effect (Fig. 6e).

It has been proposed that RAD6A–RAD18 has two biochemical functions for polymerase switching. One is mono-ubiquitination of PCNA. The other is targeting of pol η to 3′-ends by direct interaction.[6] To distinguish the respective contributions of the two functions of RAD6A–RAD18 in this *in vitro* system, we used a PCNA mutant, $PCNA^{(K164R)}$ (Fig. 6b). In the RAD6A–RAD18-independent reactions (Fig. 6b, lanes 5–7), an increase in the products of around 7 to 4 kb was observed to a similar extent as with wild-type PCNA (Fig. 6a). When RAD6A–RAD18 was introduced, no further accumulation of such products was observed (Fig. 6b, lanes 8–10 and graph). As a complementary experiment, E1 was omitted to prevent ubiquitination of PCNA in the presence of RAD6A–RAD18 (Fig. 6d). The results also demonstrated that omitting E1 (Fig. 6d, lanes 5–7) and replacement of PCNA with the mutant, $PCNA^{(K164R)}$ (Fig. 6d, lanes 11–13), reduced the amounts of such products to the same levels with each other, as compared with complete reactions (Fig. 6d, lanes 8–10 and graph). These results suggested that RAD6A–RAD18 itself could not stimulate recruitment of pol η without PCNA ubiquitination in this *in vitro* system.

To address the roles of UBZ[15] of pol η for polymerase switching, we replaced pol η with a UBZ defective mutant, pol $\eta^{(D652A)}$.[15] We detected clear accumulation of products around 7 to 4 kb with the mutant in the absence of RAD6A–RAD18 (Fig. 6c, lanes 5–7 and graph), indicating that the mutation did not affect either polymerase activity or the potential to access 3′-ends. When RAD6A–RAD18 was introduced, further accumulation of such products was not observed (Fig. 6c, lanes 8–10 and graph), demonstrating a crucial role of UBZ in stimulation of polymerase switching *in vitro*.

Discussion

In this work, we demonstrated that PCNA interacting with pol δ can act as a target for ubiquitination, and therefore, PCNA mono-ubiquitination could be coupled with DNA replication. Consequently, we could reconstitute replication-coupled switching between pol δ and pol η on a UV-irradiated template, while the results demonstrated discrepancies with currently accepted models, which have been proposed based on *in vivo* evidence, suggesting that regulatory factors could be missing in this *in vitro* system. Our results do allow us to discuss possible regulatory mechanisms of human pol switching.

Dynamic property of PCNA during the elongation phase of DNA synthesis

In this study, we demonstrated that PCNA accumulated on newly synthesized DNA during elongation. This is consistent with our previous report.[33] We have suggested that it could be a consequence of dynamic properties of pol δ previously.[33] Such a property of pol δ has been also described in other reports for mammalian[38,54] and yeast pol δ.[48,55] The general conclusion from these studies could be that pol δ is spontaneously and frequently dissociated from and associated to the 3′-ends during elongation. In our previous studies, we provided evidence that PCNA is released behind the 3′-end on such dissociation of pol δ. This is quite reasonable, because PCNA is tethered at the 3′-end by interactions with pol δ. We have also found that subsequent reloading of PCNA plays a crucial role in efficient elongation.[33] Therefore, it is rational and practical to attribute the accumulation of PCNA to its reloading during elongation. Notably, in yeast pol δ, accumulation of PCNA during DNA synthesis has been also reported.[48] However, several studies demonstrating opposite results also exist in the literature. Einolf and Guengerich have reported that processivity of mammalian pol δ calculated from kinetic parameters is quite high.[56] Recently, two studies have demonstrated stable pol δ–PCNA complexes at the 3′-ends in yeast.[57,58] The discrepancy might be attributed to a possibility that any modification(s) and/or accessory factor(s) in the respective preparations could differently affect the stability of pol δ.

Mechanisms of PCNA mono-ubiquitination

In this *in vitro* system, PCNA interacting with pol δ on DNA could be ubiquitinated efficiently so that PCNA mono-ubiquitination occurred coupled with DNA replication. In this reaction, RAD6–RAD18 probably accessed PCNA at the reverse side to the interaction with pol δ and RFC. This conclusion is supported by the finding that excess amounts of pol δ and RFC did not inhibit the ubiquitination reaction. Indeed, the Lys164 residue is found on the opposite side of the pol δ-interacting surface of PCNA.[59,60] A possible mechanism for the stimulation by pol δ and RFC could be that these proteins act to dispose PCNA on DNA with the proper geometry for catalysis. Indeed, it is known that the β-clamp of *E. coli*, the counterpart of PCNA, is tilted on DNA.[61] Tilted PCNA probably does not fit the catalytic site of RAD6–RAD18.

Our results showed that PCNA mono-ubiquitination is further stimulated by pol δ if the polymerase is actively replicating. This observation is consistent with findings in a cell-free system.[62] Importantly, the stimulation was not due to direct activation of ubiquitination reactions, but rather a consequence of multiple loading of PCNA molecules on the template, which was coupled with elongation.[33,48] Consequently, inhibition of elongation reduced the amounts of PCNA on the DNA, which also resulted in a decrease in the amount of ubiquitinated PCNA. Thus, growing 3′-ends and two conditions with stalled DNA synthesis, due to exhaustion of dNTP or DNA lesions, all appeared indistinguishable from one another in terms of biochemical actions of RFs, UEs, and pol δ. These findings indicate that factors that can recognize stalled replication itself and prevent association of RAD6A–RAD18 to moving replisome are missing in this *in vitro* system.

Mechanisms of polymerase switching

In this study, we reconstituted polymerase switching between pol δ and pol η, revealing two pathways *in vitro*. One is dependent on PCNA mono-ubiquitination and the other is independent of PCNA mono-ubiquitination, which predominates at higher concentrations of template DNA. This result suggested an intrinsic ability of pol η to access 3′-ends during replication, consistent with a previous report of a cell-free system.[63] Although our *in vitro* system revealed a mechanistic potential of pol η to access 3′-ends during replication, the PCNA mono-ubiquitination-independent pathway must be negligible *in vivo*, since genetic evidence has demonstrated the essential requirement of PCNA mono-ubiquitination for recruitment of pol η.[5,15,22,24,64,65] Importantly, Ouchida *et al.* have proposed the presence of a negative regulatory mechanism preventing inappropriate association of pol η with 3′-ends.[66] The discrepancy could be attributed to lack of protein factors involved in such a mechanism in this *in vitro* system.

The PCNA mono-ubiquitination-dependent reaction appeared at a very low concentration of 3′-end (130 pM, approximately 40 molecules/nucleus in human cells) and featured a crucial role for UBZ of pol η. The results suggest that interaction between UBZ and mono-ubiquitinated PCNA is essential for efficient bypass of one stalled 3′-end in the nucleus. Recent reports concerning yeast pol η in bypass reactions with mono-ubiquitinated PCNA have been contradictory. Polymerase activity of pol η was stimulated by mono-ubiquitinated PCNA in some but not all cases.[9,10] From our results, we consider that differences might be attributable to the assay conditions *in vitro*, depending on which of the two pathways is predominant.

Interaction between RAD6–RAD18 and pol η has been demonstrated,[6,12] and this might be responsible for recruitment to 3′-ends.[6] In the present study, however, polymerase switching was not stimulated by RAD6A–RAD18 itself when PCNA mono-ubiquitination was absent, suggesting that targeting of pol η by RAD6A–RAD18 could be coupled with PCNA ubiquitination.

Conceivable protein actions for human pol switching between pol δ and pol η in this *in vitro* system are shown in Fig. 7. The elongation complex consists of RFC, pol δ, and PCNA,[33] which could be a target for RAD6–RAD18. Usually, pol δ is not retained continuously at 3′-ends as a stable complex with PCNA; rather, it undergoes repeated association and dissociation cycles.[33,38,54] During this cycling,

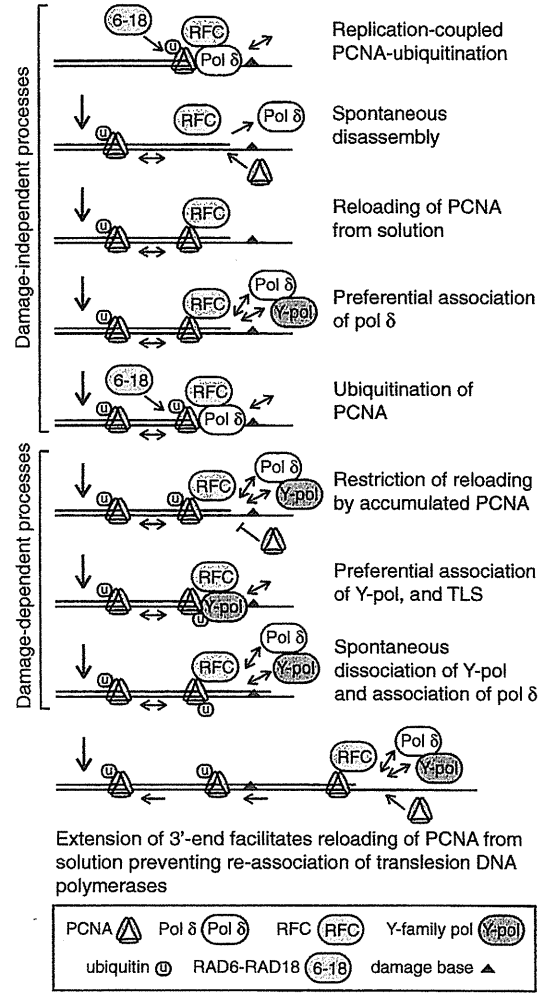

Fig. 7. Conceivable protein actions for PCNA mono-ubiquitination and polymerase switching in the present human *in vitro* system. The elongation complex consists of RFC, PCNA, and pol δ.[33] RAD6A–RAD18 preferentially ubiquitinates PCNA interacting with pol δ at a 3′-end. During association and dissociation cycles of pol δ in the growing 3′-end, the PCNA is released from the 3′-end of DNA, and new PCNA molecules are loaded from solution, preventing the pol η from association. At stalled 3′-ends, in contrast, PCNA accumulates and saturates on DNA during association and dissociation cycles of pol δ; consequently, the same PCNA molecules are repeatedly recruited to the 3′-end. Once the PCNA is ubiquitinated, it persists until association of pol η through interaction with the ubiquitinated PCNA. After DNA synthesis is restored, a fresh PCNA molecule is loaded from solution, reducing the probability of pol η access.

PCNA is released and left behind, and RFC incorporates PCNA that slides back to the 3′-end or reloads PCNA from solution.[33] These are dynamic and stochastic events. When PCNA molecules accumulate on DNA, the probability of reutilization is much higher than that of reloading from solution.[33] Thus, at growing ends, ubiquitin-free PCNA molecules normally tend to be loaded from solution. Under these circumstances, ubiquitinated PCNA molecules are not retained proximately to the 3′-ends so that pol η is restricted from association. At a stalled 3′-end, PCNA molecules are quickly accumulated onto DNA until reaching saturation. Consequently, the same PCNA molecule stays proximately to the stalled 3′-end. Once the PCNA molecule is ubiquitinated, it persists until pol η associates through interaction with the mono-ubiquitinated PCNA and extends the 3′-end. Once DNA synthesis is restored, PCNA molecules on DNA are diluted, facilitating reloading of fresh PCNA from solution and reducing the probability of pol η access.

Importantly, our results in the human system are quite different from some recent reports with a yeast system,[57,58] but not all.[48,55] In those reports,[57,58] it seems that pol δ is stably associated with PCNA during elongation but destabilizes with stalling replication. Such destabilization is more significant when PCNA is mono-ubiquitinated. Once pol η binds to ubiquitinated PCNA, association of pol δ is prohibited. Therefore, it is possible that some factors, which can stabilize pol δ–PCNA and pol η–PCNA interactions, could be missing in this human *in vitro* system.[33,37,38,54] Our system could thus be useful to address such missing factors for further understanding of molecular mechanisms of polymerase switching in humans.

Materials and Methods

Proteins

Recombinant human proteins were overproduced in *E. coli* cells and purified by conventional column chromatography. Detailed procedures for plasmid construction and protein purification are described in the Supplementary Data.

PCNA mono-ubiquitination assays

The standard reaction mixture (25 μl) contained 20 mM Hepes–NaOH (pH 7.5); 50 mM NaCl; 0.2 mg/ml bovine serum albumin (BSA); 1 mM DTT; 10 mM $MgCl_2$; 1 mM ATP; 0.1 mM each of dGTP, dATP, dCTP, and dTTP; 33 fmol of singly primed mp18 ssDNA (with the 90-mer primer, CTGCAAGGCGATTAAGTTGGGTAACGCCAGGGTTTTCCCAGTCACGACGTTGTAAAACGACGGCCAGTGCCAAGCTTGCATGCCTGCAGG); RPA (9 pmol); PCNA (1 pmol); RFC (88 fmol); E1 (850 fmol); RAD6A–RAD18 complex (950 fmol); and ubiquitin (170 pmol). Reaction mixtures were prepared on ice and then incubated at 30 °C for the indicated times. After termination of reactions with addition of 2 μl of 300 mM ethylenediaminetetraacetic acid (EDTA), the mixtures were immediately chilled on ice. Ubiquitination of PCNA was measured by Western analysis with an anti-PCNA antibody (Santa Cruz, sc-7907). Detection was carried out using an ECL chemiluminescence kit (GE Healthcare, Tokyo, Japan) and a CCD camera.

For ubiquitination assays with poly(dA)–oligo(dT), 100 ng of DNA including 900 fmol of oligo(dT) (GE Healthcare), instead of 33 fmol of mp18 DNA, was mixed under the standard reaction conditions except for the omission of dNTPs, RPA and RFC.

DNA replication assays

The standard reaction mixtures with [α-^{32}P]dTTP (25 μl) were preincubated at 30 °C for 1 min, and then reactions were started by addition of pol δ (380 fmol). After incubation at 30 °C for the indicated times, reactions were terminated with 2 μl of 300 mM EDTA, and the mixtures were immediately chilled on ice. Products of DNA synthesis were analyzed as described earlier.[33] Gel images of autoradiography were analyzed by Multi Gauge software Version 3.0 (FUJIFILM, Tokyo, Japan).

For replication assays with poly(dA)–oligo(dT), 100 ng of DNA including 900 fmol of oligo(dT) (GE Healthcare), instead of 33 fmol of mp18 DNA, was mixed under the standard reaction conditions including [α-^{32}P]dTTP, but not other dNTPs, RPA and RFC.

PCNA mono-ubiquitination of DNA–PCNA complexes isolated by gel filtration

For the introduction of nicks, plasmid pUC18 was reacted with N.BstNBI (New England BioLabs, Tokyo, Japan) at 55 °C for 60 min. Then, DNA was extracted with phenol/chloroform and precipitated with ethanol. PCNA (8 pmol), $RFC^{(p140N555)}$ (36 fmol), and the nicked plasmid pUC18 (133 fmol) were incubated at 30 °C for 15 min in 100 μl of buffer containing 20 mM Hepes–NaOH (pH 7.5), 100 mM NaCl, 0.2 mg/ml BSA, 1 mM DTT, 10 mM $MgCl_2$, and 1 mM ATP. The mixture was then immediately applied at room temperature to a 2-ml column of 4% agarose beads (A-1040-S, Agarose Beads Technologies, Madrid, Spain) equilibrated in buffer containing 20 mM Hepes–NaOH (pH 7.5), 1 mM DTT, 10 mM $MgCl_2$, and 50 mM NaCl, and fractions of three drops each were collected on ice. The fractions eluted in void volume containing DNA were pooled, and then 12.5-μl aliquots were incubated with E1 (850 fmol), RAD6A–RAD18 complex (38 fmol), and ubiquitin (170 pmol) in the presence of the indicated amounts of RFC or pol δ at 30 °C for 30 min in 25-μl reaction mixtures [20 mM Hepes–NaOH (pH 7.5), 50 mM NaCl, 0.2 mg/ml BSA, 1 mM DTT, 10 mM $MgCl_2$, 1 mM ATP, and 0.1 mM each of dGTP, dATP, and dTTP].

Isolation of PCNA on DNA bound to magnetic beads

The 5′-biotinylated primer (TCTCTCTCTCTGCAAGGCGATTAAGTTGGGTAACGCCAGGGTTTTCCCAGTCACGACGTTGTAAAACGACGGCCAGTGCCAAGCTTGCATGCCTGCAGG) was annealed to 33 fmol mp18 ssDNA and immobilized onto a 10-μl suspension of streptavidin magnetic beads, Dynabeads M280 (Life Technologies, Tokyo, Japan), as described previously.[33] Assays were carried out under standard reaction conditions as described for Fig. 4c. After termination of the reactions with 2 μl of 300 mM EDTA, the beads were washed and analyzed.[33]

Assay for PCNA mono-ubiquitination-dependent polymerase switching

RPA (900 fmol), PCNA (1 pmol), RFC (26 fmol), E1 (850 fmol), RAD6A–RAD18 complex (950 fmol), ubiquitin (170 pmol), and 3.3 fmol of singly primed mp18 ssDNA (with the 36-mer primer, CAGGGTTTTCCCAGTCACGACGTTGTAAAACGACGG) were mixed under standard reaction conditions with [α-^{32}P]dTTP in the presence or absence of pol η (10 fmol). After incubation at 30 °C for 1 min, pol δ (750 fmol) was added and the mixture was further incubated for the indicated times. Reaction products (10 μl) were analyzed by 0.7% alkaline agarose gel electrophoresis.[33] Gel images of autoradiography were analyzed by Multi Gauge software Version 3.0 (FUJIFILM).

Acknowledgements

We thank Dr. Marc S. Wold (University of Iowa College of Medicine, Iowa City, IA), Dr. Fumio Hanaoka (Osaka University, Osaka, Japan), Dr. Toshiki Tsurimoto (Kyushu University, Fukuoka, Japan), Dr. Tomohiko Ohta (St. Marianna University School of Medicine, Kanagawa, Japan), and Dr. Tadashi Shimamoto (Hiroshima University, Hiroshima, Japan) for respectively providing an RPA expression plasmid, *POLH* cDNA, a PCNA expression plasmid, a ubiquitin-encoding plasmid, and an *E. coli* strain to produce mp18 ssDNA. Several cloning vectors were obtained from the National BioResource Project (National Institute of Genetics, Japan). We also thank Dr. Niels de Wind (Leiden University Medical Center, Leiden, The Netherlands) and Dr. Hiroshi Hashimoto (Yokohama City University, Kanagawa) for their comments and suggestions on the manuscript. We are grateful to Kenji Masuda for his help with cDNA cloning and Tomoka Nakashima, Fumie Okubo, Kazumi Shimamoto, Miki Suzuki, and Mai Yoshida for their laboratory assistance. This work was supported by Grants-in-Aid from the Ministry of Education, Culture, Sports, Science and Technology of Japan (to Y.M. and K.K.); by the 21st Century Center of Excellence program from the Ministry of Education, Culture, Sports, Science and Technology of Japan (to K.K.); by Health and Labour Science Research Grants (to K.K.); by Grants-in-Aid for Cancer Research from the Ministry of Health, Labour and Welfare (to K.K.); and by the Radiation Effects Association (to Y.M.). During the performance of this work, J.P. was supported by a Japan Society for the Promotion of Science Research Fellowship for Young Scientists.

Supplementary Data

Supplementary data associated with this article can be found, in the online version, at doi:10.1016/j.jmb.2010.01.003

References

1. Hishida, T., Kubota, Y., Carr, A. M. & Iwasaki, H. (2009). *RAD6–RAD18–RAD5*-pathway-dependent tolerance to chronic low-dose ultraviolet light. *Nature*, **457**, 612–615.
2. Lehmann, A. R., Niimi, A., Ogi, T., Brown, S., Sabbioneda, S., Wing, J. F. *et al.* (2007). Translesion synthesis: Y-family polymerases and the polymerase switch. *DNA Repair (Amst.)*, **6**, 891–899.
3. Andersen, P. L., Xu, F. & Xiao, W. (2008). Eukaryotic DNA damage tolerance and translesion synthesis through covalent modifications of PCNA. *Cell Res.* **18**, 162–173.
4. Hoege, C., Pfander, B., Moldovan, G. L., Pyrowolakis, G. & Jentsch, S. (2002). RAD6-dependent DNA repair is linked to modification of PCNA by ubiquitin and SUMO. *Nature*, **419**, 135–141.
5. Stelter, P. & Ulrich, H. D. (2003). Control of spontaneous and damage-induced mutagenesis by SUMO and ubiquitin conjugation. *Nature*, **425**, 188–191.
6. Watanabe, K., Tateishi, S., Kawasuji, M., Tsurimoto, T., Inoue, H. & Yamaizumi, M. (2004). Rad18 guides polη to replication stalling sites through physical interaction and PCNA monoubiquitination. *EMBO J.* **23**, 3886–3896.
7. Bailly, V., Lamb, J., Sung, P., Prakash, S. & Prakash, L. (1994). Specific complex formation between yeast RAD6 and RAD18 proteins: a potential mechanism for targeting RAD6 ubiquitin-conjugating activity to DNA damage sites. *Genes Dev.* **8**, 811–820.
8. Bailly, V., Lauder, S., Prakash, S. & Prakash, L. (1997). Yeast DNA repair proteins Rad6 and Rad18 form a heterodimer that has ubiquitin conjugating, DNA binding, and ATP hydrolytic activities. *J. Biol. Chem.* **272**, 23360–23365.
9. Garg, P. & Burgers, P. M. (2005). Ubiquitinated proliferating cell nuclear antigen activates translesion DNA polymerases η and REV1. *Proc. Natl Acad. Sci. USA*, **102**, 18361–18366.
10. Haracska, L., Unk, I., Prakash, L. & Prakash, S. (2006). Ubiquitylation of yeast proliferating cell nuclear antigen and its implications for translesion DNA synthesis. *Proc. Natl Acad. Sci. USA*, **103**, 6477–6482.
11. Xin, H., Lin, W., Sumanasekera, W., Zhang, Y., Wu, X. & Wang, Z. (2000). The human *RAD18* gene product interacts with HHR6A and HHR6B. *Nucleic Acids Res.* **28**, 2847–2854.
12. Yuasa, M. S., Masutani, C., Hirano, A., Cohn, M. A., Yamaizumi, M., Nakatani, Y. & Hanaoka, F. (2006). A human DNA polymerase η complex containing Rad18, Rad6 and Rev1; proteomic analysis and targeting of the complex to the chromatin-bound fraction of cells undergoing replication fork arrest. *Genes Cells*, **11**, 731–744.
13. Unk, I., Hajdu, I., Fatyol, K., Szakal, B., Blastyak, A., Bermudez, V. *et al.* (2006). Human SHPRH is a ubiquitin ligase for Mms2-Ubc13-dependent polyubiquitylation of proliferating cell nuclear antigen. *Proc. Natl Acad. Sci. USA*, **103**, 18107–18112.
14. Bi, X., Barkley, L. R., Slater, D. M., Tateishi, S., Yamaizumi, M., Ohmori, H. & Vaziri, C. (2006). Rad18 regulates DNA polymerase κ and is required for recovery from S-phase checkpoint-mediated arrest. *Mol. Cell. Biol.* **26**, 3527–3540.
15. Bienko, M., Green, C. M., Crosetto, N., Rudolf, F., Zapart, G., Coull, B. *et al.* (2005). Ubiquitin-binding domains in Y-family polymerases regulate translesion synthesis. *Science*, **310**, 1821–1824.

16. Guo, C., Tang, T. S., Bienko, M., Parker, J. L., Bielen, A. B., Sonoda, E. *et al.* (2006). Ubiquitin-binding motifs in REV1 protein are required for its role in the tolerance of DNA damage. *Mol. Cell. Biol.* **26**, 8892–8900.
17. Kannouche, P. L., Wing, J. & Lehmann, A. R. (2004). Interaction of human DNA polymerase η with monoubiquitinated PCNA: a possible mechanism for the polymerase switch in response to DNA damage. *Mol. Cell*, **14**, 491–500.
18. Plosky, B. S., Vidal, A. E., Fernandez de Henestrosa, A. R., McLenigan, M. P., McDonald, J. P., Mead, S. & Woodgate, R. (2006). Controlling the subcellular localization of DNA polymerases ι and η via interactions with ubiquitin. *EMBO J.* **25**, 2847–2855.
19. Motegi, A., Sood, R., Moinova, H., Markowitz, S. D., Liu, P. P. & Myung, K. (2006). Human SHPRH suppresses genomic instability through proliferating cell nuclear antigen polyubiquitination. *J. Cell Biol.* **175**, 703–708.
20. Motegi, A., Liaw, H. J., Lee, K. Y., Roest, H. P., Maas, A., Wu, X. *et al.* (2008). Polyubiquitination of proliferating cell nuclear antigen by HLTF and SHPRH prevents genomic instability from stalled replication forks. *Proc. Natl Acad. Sci. USA*, **105**, 12411–12416.
21. Unk, I., Hajdu, I., Fatyol, K., Hurwitz, J., Yoon, J. H., Prakash, L. *et al.* (2008). Human HLTF functions as a ubiquitin ligase for proliferating cell nuclear antigen polyubiquitination. *Proc. Natl Acad. Sci. USA*, **105**, 3768–3773.
22. Arakawa, H., Moldovan, G. L., Saribasak, H., Saribasak, N. N., Jentsch, S. & Buerstedde, J. M. (2006). A role for PCNA ubiquitination in immunoglobulin hypermutation. *PLoS Biol.* **4**, e366.
23. Edmunds, C. E., Simpson, L. J. & Sale, J. E. (2008). PCNA ubiquitination and REV1 define temporally distinct mechanisms for controlling translesion synthesis in the avian cell line DT40. *Mol. Cell*, **30**, 519–529.
24. Langerak, P., Nygren, A. O., Krijger, P. H., van den Berk, P. C. & Jacobs, H. (2007). A/T mutagenesis in hypermutated immunoglobulin genes strongly depends on $PCNA^{K164}$ modification. *J. Exp. Med.* **204**, 1989–1998.
25. Delbos, F., De Smet, A., Faili, A., Aoufouchi, S., Weill, J. C. & Reynaud, C. A. (2005). Contribution of DNA polymerase η to immunoglobulin gene hypermutation in the mouse. *J. Exp. Med.* **201**, 1191–1196.
26. Martomo, S. A., Yang, W. W., Wersto, R. P., Ohkumo, T., Kondo, Y., Yokoi, M. *et al.* (2005). Different mutation signatures in DNA polymerase η- and MSH6-deficient mice suggest separate roles in antibody diversification. *Proc. Natl Acad. Sci. USA*, **102**, 8656–8661.
27. Zeng, X., Winter, D. B., Kasmer, C., Kraemer, K. H., Lehmann, A. R. & Gearhart, P. J. (2001). DNA polymerase η is an A–T mutator in somatic hypermutation of immunoglobulin variable genes. *Nat. Immunol.* **2**, 537–541.
28. Frampton, J., Irmisch, A., Green, C. M., Neiss, A., Trickey, M., Ulrich, H. D. *et al.* (2006). Postreplication repair and PCNA modification in *Schizosaccharomyces pombe*. *Mol. Biol. Cell*, **17**, 2976–2985.
29. Simpson, L. J., Ross, A. L., Szuts, D., Alviani, C. A., Oestergaard, V. H., Patel, K. J. & Sale, J. E. (2006). RAD18-independent ubiquitination of proliferating-cell nuclear antigen in the avian cell line DT40. *EMBO Rep.* **7**, 927–932.
30. Huang, T. T., Nijman, S. M., Mirchandani, K. D., Galardy, P. J., Cohn, M. A., Haas, W. *et al.* (2006). Regulation of monoubiquitinated PCNA by DUB autocleavage. *Nat. Cell Biol.* **8**, 339–347.
31. Oestergaard, V. H., Langevin, F., Kuiken, H. J., Pace, P., Niedzwiedz, W., Simpson, L. J. *et al.* (2007). Deubiquitination of FANCD2 is required for DNA crosslink repair. *Mol. Cell*, **28**, 798–809.
32. Davies, A. A., Huttner, D., Daigaku, Y., Chen, S. & Ulrich, H. D. (2008). Activation of ubiquitin-dependent DNA damage bypass is mediated by replication protein A. *Mol. Cell*, **29**, 625–636.
33. Masuda, Y., Suzuki, M., Piao, J., Gu, Y., Tsurimoto, T. & Kamiya, K. (2007). Dynamics of human replication factors in the elongation phase of DNA replication. *Nucleic Acids Res.* **35**, 6904–6916.
34. Zuo, S., Bermudez, V., Zhang, G., Kelman, Z. & Hurwitz, J. (2000). Structure and activity associated with multiple forms of *Schizosaccharomyces pombe* DNA polymerase δ. *J. Biol. Chem.* **275**, 5153–5162.
35. Burgers, P. M. & Gerik, K. J. (1998). Structure and processivity of two forms of *Saccharomyces cerevisiae* DNA polymerase δ. *J. Biol. Chem.* **273**, 19756–19762.
36. Lee, M. Y., Tan, C. K., Downey, K. M. & So, A. G. (1984). Further studies on calf thymus DNA polymerase δ purified to homogeneity by a new procedure. *Biochemistry*, **23**, 1906–1913.
37. Podust, L. M., Podust, V. N., Sogo, J. M. & Hübscher, U. (1995). Mammalian DNA polymerase auxiliary proteins: analysis of replication factor C-catalyzed proliferating cell nuclear antigen loading onto circular double-stranded DNA. *Mol. Cell. Biol.* **15**, 3072–3081.
38. Podust, V. N., Chang, L. S., Ott, R., Dianov, G. L. & Fanning, E. (2002). Reconstitution of human DNA polymerase δ using recombinant baculoviruses: the p12 subunit potentiates DNA polymerizing activity of the four-subunit enzyme. *J. Biol. Chem.* **277**, 3894–3901.
39. Tsurimoto, T. & Stillman, B. (1991). Replication factors required for SV40 DNA replication *in vitro*. I. DNA structure-specific recognition of a primer-template junction by eukaryotic DNA polymerases and their accessory proteins. *J. Biol. Chem.* **266**, 1950–1960.
40. Fukuda, K., Morioka, H., Imajou, S., Ikeda, S., Ohtsuka, E. & Tsurimoto, T. (1995). Structure–function relationship of the eukaryotic DNA replication factor, proliferating cell nuclear antigen. *J. Biol. Chem.* **270**, 22527–22534.
41. Tsurimoto, T., Shinozaki, A., Yano, M., Seki, M. & Enomoto, T. (2005). Human Werner helicase interacting protein 1 (WRNIP1) functions as a novel modulator for DNA polymerase δ. *Genes Cells*, **10**, 13–22.
42. Shikata, K., Ohta, S., Yamada, K., Obuse, C., Yoshikawa, H. & Tsurimoto, T. (2001). The human homologue of fission Yeast cdc27, p66, is a component of active human DNA polymerase δ. *J. Biochem.* **129**, 699–708.
43. Burgers, P. M. & Yoder, B. L. (1993). ATP-independent loading of the proliferating cell nuclear antigen requires DNA ends. *J. Biol. Chem.* **268**, 19923–19926.
44. Uhlmann, F., Cai, J., Gibbs, E., O'Donnell, M. & Hurwitz, J. (1997). Deletion analysis of the large subunit p140 in human replication factor C reveals regions required for complex formation and replication activities. *J. Biol. Chem.* **272**, 10058–10064.
45. Podust, V. N., Tiwari, N., Stephan, S. & Fanning, E. (1998). Replication factor C disengages from proliferating cell nuclear antigen (PCNA) upon sliding clamp formation, and PCNA itself tethers DNA polymerase δ to DNA. *J. Biol. Chem.* **273**, 31992–31999.

46. Yao, N., Turner, J., Kelman, Z., Stukenberg, P. T., Dean, F., Shechter, D. *et al.* (1996). Clamp loading, unloading and intrinsic stability of the PCNA, β and gp45 sliding clamps of human, *E. coli* and T4 replicases. *Genes Cells*, **1**, 101–113.
47. Yuzhakov, A., Kelman, Z., Hurwitz, J. & O'Donnell, M. (1999). Multiple competition reactions for RPA order the assembly of the DNA polymerase δ holoenzyme. *EMBO J.* **18**, 6189–6199.
48. Chilkova, O., Stenlund, P., Isoz, I., Stith, C. M., Grabowski, P., Lundstrom, E. B. *et al.* (2007). The eukaryotic leading and lagging strand DNA polymerases are loaded onto primer-ends via separate mechanisms but have comparable processivity in the presence of PCNA. *Nucleic Acids Res.* **35**, 6588–6597.
49. Masutani, C., Kusumoto, R., Yamada, A., Dohmae, N., Yokoi, M., Yuasa, M. *et al.* (1999). The *XPV* (xeroderma pigmentosum variant) gene encodes human DNA polymerase η. *Nature*, **399**, 700–704.
50. Masutani, C., Araki, M., Yamada, A., Kusumoto, R., Nogimori, T., Maekawa, T. *et al.* (1999). Xeroderma pigmentosum variant (XP-V) correcting protein from HeLa cells has a thymine dimer bypass DNA polymerase activity. *EMBO J.* **18**, 3491–3501.
51. Haracska, L., Johnson, R. E., Unk, I., Phillips, B., Hurwitz, J., Prakash, L. & Prakash, S. (2001). Physical and functional interactions of human DNA polymerase η with PCNA. *Mol. Cell. Biol.* **21**, 7199–7206.
52. Haracska, L., Kondratick, C. M., Unk, I., Prakash, S. & Prakash, L. (2001). Interaction with PCNA is essential for yeast DNA polymerase η function. *Mol. Cell*, **8**, 407–415.
53. Kusumoto, R., Masutani, C., Shimmyo, S., Iwai, S. & Hanaoka, F. (2004). DNA binding properties of human DNA polymerase η: implications for fidelity and polymerase switching of translesion synthesis. *Genes Cells*, **9**, 1139–1150.
54. Tsurimoto, T. & Stillman, B. (1989). Multiple replication factors augment DNA synthesis by the two eukaryotic DNA polymerases, α and δ. *EMBO J.* **8**, 3883–3889.
55. McCulloch, S. D., Kokoska, R. J., Garg, P., Burgers, P. M. & Kunkel, T. A. (2009). The efficiency and fidelity of 8-oxo-guanine bypass by DNA polymerases δ and η. *Nucleic Acids Res.* **37**, 2830–2840.
56. Einolf, H. J. & Guengerich, F. P. (2000). Kinetic analysis of nucleotide incorporation by mammalian DNA polymerase δ. *J. Biol. Chem.* **275**, 16316–16322.
57. Langston, L. D. & O'Donnell, M. (2008). DNA polymerase δ is highly processive with proliferating cell nuclear antigen and undergoes collision release upon completing DNA. *J. Biol. Chem.* **283**, 29522–29531.
58. Zhuang, Z., Johnson, R. E., Haracska, L., Prakash, L., Prakash, S. & Benkovic, S. J. (2008). Regulation of polymerase exchange between Polη and Polδ by monoubiquitination of PCNA and the movement of DNA polymerase holoenzyme. *Proc. Natl Acad. Sci. USA*, **105**, 5361–5366.
59. Gulbis, J. M., Kelman, Z., Hurwitz, J., O'Donnell, M. & Kuriyan, J. (1996). Structure of the C-terminal region of p21(WAF1/CIP1) complexed with human PCNA. *Cell*, **87**, 297–306.
60. Jonsson, Z. O., Hindges, R. & Hübscher, U. (1998). Regulation of DNA replication and repair proteins through interaction with the front side of proliferating cell nuclear antigen. *EMBO J.* **17**, 2412–2425.
61. Georgescu, R. E., Kim, S. S., Yurieva, O., Kuriyan, J., Kong, X. P. & O'Donnell, M. (2008). Structure of a sliding clamp on DNA. *Cell*, **132**, 43–54.
62. Schmutz, V., Wagner, J., Janel-Bintz, R., Fuchs, R. P. & Cordonnier, A. M. (2007). Requirements for PCNA monoubiquitination in human cell-free extracts. *DNA Repair (Amst.)*, **6**, 1726–1731.
63. Bebenek, K., Matsuda, T., Masutani, C., Hanaoka, F. & Kunkel, T. A. (2001). Proofreading of DNA polymerase η-dependent replication errors. *J. Biol. Chem.* **276**, 2317–2320.
64. Acharya, N., Yoon, J. H., Gali, H., Unk, I., Haracska, L., Johnson, R. E. *et al.* (2008). Roles of PCNA-binding and ubiquitin-binding domains in human DNA polymerase η in translesion DNA synthesis. *Proc. Natl Acad. Sci. USA*, **105**, 17724–17729.
65. Parker, J. L., Bielen, A. B., Dikic, I. & Ulrich, H. D. (2007). Contributions of ubiquitin- and PCNA-binding domains to the activity of polymerase η in *Saccharomyces cerevisiae*. *Nucleic Acids Res.* **35**, 881–889.
66. Ouchida, R., Ukai, A., Mori, H., Kawamura, K., Dolle, M. E., Tagawa, M. *et al.* (2008). Genetic analysis reveals an intrinsic property of the germinal center B cells to generate A:T mutations. *DNA Repair (Amst.)*, **7**, 1392–1398.

Paternal monoenergetic neutron exposure results in abnormal sperm, and embryonal lethality and transgenerational tumorigenesis in mouse F_1 offspring

HIROMITSU WATANABE[1], MEGUMI TOYOSHIMA[1], MASAYORI ISHIKAWA[2] and KENJI KAMIYA[1]

[1]Department of Experimental Oncology, Research Institute for Radiation Biology and Medicine, Hiroshima University, Kasumi 1-2-3, Minami-ku, Hiroshima 734-8553; [2]Department of Molecular Trace Radiation Medicine, Hokkaido University Hospital, North 15 West 7, Kita-ku, Sapporo 060-8648, Japan

Received December 2, 2009; Accepted January 28, 2010

DOI: 10.3892/or_00000771

Abstract. Experiments were conducted to assay whether monoenergetic neutron-induced genetic damage in parental germline cells can give rise to development of cancer in the offspring. Seven-week-old C3H male mice were irradiated with monoenergetic neutrons with energy levels of 0.2 or 0.6 MeV at doses of 0, 50, 100 or 200 cGy. Two weeks after irradiation, when the male mice showed an increased incidence of sperm abnormalities, they were mated with virgin 9-week-old C57BL females. Litter size was decreased and embryo lethalities were increased in a dose-dependent manner. Furthermore, tumor incidence in male offspring born to male mice irradiated with 25 or 50 cGy at 0.6 MeV showed a tendency for increase as compared to the non-irradiated group value. Liver tumors in the 50 cGy group were significantly increased (P=0.03). It is concluded that the increased hepatic tumor risk in the F_1 generation may have been caused by genetic transmission of some hepatoma-associated trait(s) induced by monoenergetic neutron irradiation.

Introduction

There is now a wealth of information on the transmission of tumor-related genetic traits through germ cells from parents to offspring and research has been performed to address this question not only in man but also experimental animals (1-3). The possible importance of such genetic transmission is evidenced by the finding of increased risk of leukemia and non-Hodgkin lymphoma in children of workers at the Sellafield nuclear plant and in the West Berkshire and North Hampshine nuclear industries (4). Furthermore, experimental evidence for germinal transmission of cancer-related genetic damage has been obtained after parental exposure to ethylnitrosourea (5), X-rays and urethane (6) and neutron irradiation (7-9).

In order to study the radiobiological effects of neutron, the Hiroshima University Radiobiological Research Accelerator (HIRRAC) can be operated under conditions of high proton beam currents of 1 mA and acceleration voltages up to 3 MeV. The biological effects of monoenergetic neutrons are of particular interest to basic science and radiation protection (10). Concern is reflected in *in vitro* assays (11-17) as well as *in vivo* studies (18). To our knowledge, however, there has been relatively little work on the genetic effects of monoenergetic neutrons at various energy levels using *in vivo* systems.

Specifications for biological irradiation are presented in terms of monoenergetic beam conditions, dose rates and deposited energy spectra. High dose rates of monoenergetic neutron fields are useful for studying the neutron energy dependency of biological effects, and also for other radiobiology studies on the basic mechanisms of the effects of neutrons. Monoenergetic neutrons which have a narrow neutron spectrum are the most useful, therefore they were chosen for the present study of whether irradiation-induced genetic damage can be passed to the offspring, causing embryonic lethality and tumor development in the F_1 generation.

Materials and methods

Animals. COBOS male C3H/HeNCrj and female C57BL/6NCrj mice were purchased from Charles River Japan, Inc. (Hino, Japan) and housed in autoclaved cages on sterile wood chips, in a room with controlled temperature (24±2°C), humidity (55±10%) and a regular 12-h light, 12-h dark cycle, under the guidelines set forth in the 'Guide for the Care and Use of Laboratory Animals' established by Hiroshima University. They were fed a commercial diet MF (Oriental Yeast Co., Ltd., Tokyo, Japan) and were provided with normal tap water *ad libitum*. All experiments used the same lot of animals.

Correspondence to: Dr Hiromitsu Watanabe, Department of Experimental Oncology, Research Institute for Radiation Biology and Medicine, Hiroshima University, 1-2-3 Kasumi, Minami-ku, Hiroshima 734-8553, Japan
E-mail: tonko@hiroshima-u.ac.jp

Key words: monoenergetic neutrons, mouse, paternal exposure, offspring, tumorigenesis

Table I. Body, testis, epididymis weights and abnormal sperm induced 3 weeks after monoenegic neutron.

	BW	Testis	Epididymis	Testis/BW	Epi/bw	Sperm abnormal
0 cGy	28.9±1.9	0.17±0.02	0.063±0.006	6.01±0.76	2.21±0.20	1.56±0.76
0.2 MeV						
12.5 cGy	27.9±1.0	0.13±0.01[a]	0.062±0.007	4.69±0.47[a]	2.22±0.22	0.96±0.33
25 cGy	28.0±1.0	0.11±0.02[a]	0.056±0.004[a]	3.80±0.55[a]	2.01±0.16	1.93±1.08
50 cGy	27.9±1.3	0.10±0.01[a]	0.054±0.003[a]	3.46±0.17[a]	1.95±0.12[b]	1.92±1.18
100 cGy	26.7±1.2[a]	0.08±0.01[a]	0.053±0.005[a]	2.92±0.34[a]	1.97±0.23[b]	4.06±1.16[a]
		Y=-0.078X+0.14		Y=-0.026X+5.2		Y=0.026X+1.07
		r^2=-0.90		r^2=-0.89		r^2=0.92
		P<0.05		P<0.05		P<0.05
0.6 MeV						
12.5 cGy	27.7±1.1	0.13±0.01[a]	0.061±0.006	4.70±0.35[a]	2.19±0.20	1.50±0.65
25 cGy	29.3±1.9	0.11±0.01[a]	0.061±0.027	3.66±0.37[a]	2.10±0.21	2.36±1.66
50 cGy	28.0±1.3	0.09±0.01[a]	0.057±0.002[b]	3.36±0.33[a]	2.02±0.09	3.07±1.43[b]
100 cGy	27.5±1.1[b]	0.08±0.01[a]	0.055±0.005[a]	2.91±0.18[a]	1.98±0.20[b]	6.18±1.07[a,c]
		Y=-0.078X+0.14		Y=-0.026X+5.1		Y=0.048X+1.14
		r^2=-0.86		r^2=-0.84		r^2=0.98
						P<0.01

(Mean ± SD). [a]Significantly different from 0 cGy value (P<0.01). [b]Significantly different from 0 cGy value (P<0.05). [c]Significantly different from 0.2 MeV 100 cGy value (P<0.01).

Monoenergetic neutron irradiation. Neutron sources in this study was produced by Hiroshima University Radiobiological Research Accelerator (HIRRAC) as described previously (18). The HIRRAC can generate various monoenergetic neutrons using ^{7}Li(p,n)^{7}Be reaction with maximum accelerated voltage of 3 MV.

The absorbed doses were evaluated using paired ionization chambers IC-17 ATW (FWT, Inc., Goleta, CA, USA) and IC-17G (model GM539, FWT, Inc.). The IC-17ATW, which is made of tissue equivalent materials and filled with propane-base tissue equivalent gas, can measure the sum of neutron and γ-ray dose. The IC-17G, which is made of carbon and filled with carbon dioxide gas, can measure γ-ray dose with a few neutron dose contributions. Using these chambers, separate dose of neutron and γ-ray can be evaluated. The γ-ray contamination was estimated <3% of neutron dose when using 10-μm-thick lithium targets.

Each mouse was put into a box (3 cm x 3 cm x 5 cm) and 5 mice were located 20 cm away from target plane and 10 cm away from beam axis, which means that the mice were placed at 30 degrees direction position.

In order to uniform individual neutron doses, mice were rotated with a speed of 1 rpm. Groups of 5 mice were exposed by monoernergetic neutrons in 0.20 and 0.6 MeV (dose 50 cGy, dose rate 0.5 cGy/min) without anesthesia. The accelerated voltages for their neutron energy were 2.0 and 2.37 MV, respectively.

Experiments. One hundred and ten male mice received a single whole body exposure to monoernergetic neutrons with energy levels of 0.2 or 0.6 MeV at doses of 0, 25, 50, 100 or 200 cGy. Two weeks (spermatid stage) after irradiation, the males were mated with 3 non-irradiated 9-week-old C57BL female mice for a week, and retired males were then sacrificed. Testes were minced in saline and filtered and sperm were stained with Giemsa solution to allow the numbers of normal and abnormal sperm to be counted (19).

A total of 47 successfully mated females in one group were sacrificed 18 days after fertilization and the numbers of surviving and dead embryos were counted. In the remainder, offspring were obtained, the ratio of surviving pups was determined 1 week after birth, and the F_1 mice were maintained until 13.5 months of age.

Pathology. All animals were regularly observed on a daily basis and weighed once a month. At the time of necropsy, full autopsies were carried out under ether anesthesia, and body weights and various organ weights were determined. The number and size of liver tumor nodules were also measured and diseases of the liver and other organs including neoplastic changes were diagnosed by routine histological examination.

Statistical analysis. The significance of differences in numerical data was determined using the χ^2, Student's t-tests and the Dunnett method for multiple comparisons using logarithmic transformation.

Results

Changes in body and organ weights and appearance of abnormal sperm in the irradiated mice. Body weights of

Table II. Females mice used.

	Used females	Non-pregnancy	Pregnancy			
			Used for embryo lethality	Non-nursing	Nursing (%)	Total
0 cGy	37	15 (41)	4	1 (6)	17 (94)	18
0.2 MeV						
12.5 cGy	20	6 (30)	8	0	6 (100)	6
25 cGy	15	5 (33)	3	1 (14)	6 (86)	7
50 cGy	16	3 (19)	5	0	8 (100)	8
100 cGy	16	5 (31)	4	2 (29)	5 (71)	7
0.6 MeV						
12.5 cGy	19	7 (37)	7	1 (20)	4 (80)	5
25 cGy	20	4 (20)	8	1 (13)	7 (88)	8
50 cGy	15	5 (33)	3	0	7 (100)	7
100 cGy	37	16 (43)	5	11 (65)	6 (35)	17

100 cGy irradiated males with both energies were significantly decreased as compared with non-irradiated controls. Testis absolute (in 0.2 MeV $Y=-0.078X+0.14$, $r^2=-0.90$, $P<0.05$; in 0.6 MeV $Y=-0.078X+0.14$, $r^2=-0.86$) and relative weights (in 0.2 MeV $Y=-0.026X+5.2$, $r^2=-0.89$, $P<0.05$); in 0.6 MeV $Y=-0.26X+5.1$, $r^2=-0.84$) were also decreased linearly. The epididymis weights were decreased. Ratios of abnormal sperm were increased and with 100 cGy at 0.6 MeV the value was significantly greater than with 0.2 MeV (Table I) (0.2 MeV $Y=0.026X+1.07$, $r^2=0.92$, $P<0.05$; in 0.6 MeV $Y=0.048X+1.14$, $r^2=0.98$, $P<0.01$).

Survival of embryos. Data for used female mice are shown in Table II. Non-pregnant females accounted for 19-43%. Numbers of implantations per mouse were decreased in a dose-dependent manner (Table III 0.2 MeV $Y=-0.035X+8.78$, $r^2=-0.91$, $P<0.05$; in 0.6 MeV $Y=-0.034X+93$, $r^2=-0.90$, $P<0.05$). Numbers of total embryos in 100 cGy with both energy levels were significantly decreased as compared with other dose groups (Table III). Numbers of surviving embryos were significantly lower with 100 cGy irradiation with the average numbers of surviving embryos per mother were decreased in a dose-dependent manner (in 0.2 MeV $Y=-0.058X+7.5$, $r^2=-0.99$, $P<0.01$; in 0.6 MeV $Y=-0.045X+7.6$, $r^2=-0.97$, $P<0.01$). Conversely, lethality increased with the dose (in 0.2 MeV $Y=0.02X+1.57$, $r^2=0.91$, $P<0.05$; in 0.6 MeV $Y=0.01X+1.71$, $r^2=0.65$).

Table III. Mean survival data for embryos.

Group	Survival	Lethal	Total
0 cGy	7.50±1.00[a,c]	1.50±1.00	9.00±1.15[a,c]
0.2 MeV			
12.5 cGy	6.50±1.20[a,c]	1.38±1.30	7.88±0.99[a,c]
25 cGy	5.00±2.00[b]	2.67±2.52	7.67±0.58[b]
50 cGy	5.20±2.28[a]	2.60±2.07	7.80±1.30[a,d]
100 cGy	1.50±1.29[e]	3.50±1.29	5.00±2.00[e]
	$Y=-0.058X+7.5$	$Y=0.02X+1.57$	$Y=-0.035X+8.78$
	$r^2=-0.99$, $P<0.01$	$r^2=0.91$, $P<0.05$	$r^2=-0.91$, $P<.0.05$
0.6 MeV			
12.5 cGy	7.43±1.72[a,c]	1.43±1.27	8.86±1.57[a,c]
25 cGy	5.75±2.05[a,d]	2.23±1.30	8.13±1.36[a,c]
50 cGy	5.67±0.58[a]	3.00±2.00	8.67±1.53[a,c]
100 cGy	3.00±1.22[e]	2.40±1.52	5.40±0.55[e]
	$Y=-0.045X+7.6$	$Y=0.01X+1.71$	$Y=-0.034X+9.3$
	$r^2=0.97$, $P<0.01$	$r^2=0.65$	$r^2=-0.90$, $P<0.05$

(Mean ± SD). [a]Significantly difference from 0.2 MeV 100 cGy value ($P<0.01$). [b]Significantly difference from 0.2 MeV 100 cGy value ($P<0.05$). [c]Significantly difference from 0.6 MeV 100 cGy value ($P<0.01$). [d]Significantly difference from 0.6 MeV 100 cGy value ($P<0.05$). [e]Significantly difference from 0 cGy value ($P<0.01$).

Birth rate and offspring nursing rate. Data for non-nursing mothers are given in Table II. The number was increased with 100 cGy at the 0.6 MeV energy level.

Offspring from mating two weeks after irradiation. Data for litter size and sex ratios are given in Table IV. Mean offspring number per mother was decreased dose-dependently at the 0.2 MeV energy level (total pups $Y=-0.05X+8.3$, $r^2=-0.99$, $P<0.01$; male $Y=-0.03X+4.0$, $r^2=-0.96$, $P<0.01$; female $Y=-0.024X+4.2$, $r^2=-0.94$, $P<0.05$) and with 0.6 MeV (total $Y=-0.06X+8.0$, $r^2=-0.97$, $P<0.01$; female $Y=-0.04X+4.4$, $r^2=-0.86$) except in males ($Y=-0.01X+2.8$, $r^2=-0.57$). The sex ratio at 0.2 MeV was about 50:50 but at 0.6 MeV differed with 12.5 cGy. In the long-term study, total number of offspring with 100 cGy at both energy levels was small.

Sequential assessment showed significant increase in body weights with 50 cGy at 0.2 MeV during 4-7 months and with 50 cGy at 0.6 MeV during to 12 months in males as

Table IV. Sex ratio after birth and effective animals.

Group	Sex ratio			No. of animals		
	Total	Male	Female	Total	Male (%)	Female (%)
0 cGy	8.53±1.37	4.53±1.37	3.88±1.73	138	74 (54)	64 (46)
0.2 MeV						
12.5 cGy	7.33±1.51	3.33±1.63	4.00±1.26	47	24 (51)	23 (49)
25 cGy	7.33±1.21	3.17±0.98	4.17±0.75	43	21 (49)	22 (51)
50 cGy	5.38±1.85[a]	2.63±0.92[a]	2.75±1.28	40	20 (50)	20 (50)
100 cGy	3.20±0.84[a]	1.40±0.89[a]	1.80±0.84[b]	16	7 (44)	9 (56)
	Y=-0.05X+8.3	Y=-0.03X+4.0	Y=-0.024X+4.22			
	r^2=-0.99, P<0.01	r^2=-0.96, P<0.01	r^2=-0.94, P<0.05			
0.6 MeV						
12.5 cGy	7.50±1.9	2.50±2.38[b]	5.00±2.16	29	10 (34)	19 (66)
25 cGy	6.00±1.63[a]	2.29±1.25[a]	3.71±1.60	38	16 (42)	22 (58)
50 cGy	4.43±0.98[a]	3.14±1.21	1.29±1.11[a]	42	22 (52)	20 (48)
100 cGy	2.50±1.22[a]	1.50±0.84[a]	1.00±0.63[a]	17	8 (47)	9 (53)
	Y=-0.06X+8.0	Y=-0.01X+2.8	Y=-0.04X+4.4			
	r^2=-0.97, P<0.01	r^2=-0.57	r^2=-0.86			

(Mean ± SD). [a]Significantly different from 0 cGy value (P<0.01). [b]Significantly different from 0 cGy value (P<0.05).

Table V. Body weights of F_1 male mice.

Group	3 months	4 months	5 months	6 months	7 months	8 months	9 months	10 months	11 months	12 months	13 months	14.5 months
0 cGy	32.1±2.7	34.2±3.4	38.2±4.0	40.0±3.9	40.8±4.2	42.7±1.9	44.3±3.4	45.2±3.1	46.2±3.3	46.8±3.6	46.8±3.4	46.0±3.4
0.2 MeV												
12.5 cGy	30.7±2.9	32.8±3.5	35.4±4.5[b]	37.1±4.9[b]	39.2±5.1	41.0±5.0	42.3±4.7	43.5±4.3	44.6±4.0	45.8±4.0	45.6±3.1	45.1±3.8
25 cGy	30.8±2.5	33.0±3.4	36.1±4.3	37.0±4.1[b]	38.3±4.3[b]	40.0±4.2[b]	41.3±4.2[a]	42.5±4.0[b]	43.6±4.0[b]	44.4±4.1[b]	45.2±4.1	44.5±4.1
50 cGy	33.8±2.7	37.5±3.6[a]	40.8±3.2[b]	42.1±3.1[b]	43.4±2.9[b]	44.2±2.7	45.2±2.9	46.0±3.0	47.3±3.1	48.1±2.9	48.1±3.9	47.6±3.2
100 cGy	32.5±0.9	34.8±2.0	38.0±3.2	41.6±4.5	44.2±4.5	45.7±2.9	47.0±2.7	47.2±2.2	48.4±1.8	48.6±1.7	46.6±3.9	45.2±2.2
0.6 MeV												
12.5 cGy	31.7±1.4	33.8±2.5	37.4±3.0	38.5±3.1	41.4±4.1	41.9±3.2	43.3±3.1	44.2±2.1	45.8±2.0	46.5±3.0	46.0±3.4	45.0±3.8
25 cGy	31.7±2.3	35.1±3.1	38.5±3.9	40.4±3.0	42.7±3.5	43.9±2.8	45.7±2.8	46.7±2.8	47.9±2.9	48.3±3.3	48.8±3.6	48.1±4.0
50 cGy	32.1±4.2	36.8±4.3[b]	41.1±4.1[b]	42.8±3.8[a]	44.2±3.1[a]	46.1±3.0[a]	47.4±3.4[a]	47.7±4.5[b]	49.6±3.8[a]	49.2±3.7[b]	48.9±3.5	47.8±3.4
100 cGy	31.6±4.1	34.9±5.5	38.6±5.9	40.0±5.7	40.4±5.1	42.2±5.7	43.4±5.5	44.0±6.2	45.6±6.0	45.4±5.3	46.2±5.9	45.3±5.6

(Mean ± SD). [a]Significantly different from 0 cGy value (P<0.01). [b]Significantly different from 0 cGy value (P<0.05).

compared to control males (Table V), whereas significantly decrease was evident with 25 cGy at 0.2 MeV. Female body weights were significantly heavier than for controls with 50 cGy at 0.2 MeV from 3 to 6 months, with 100 cGy at 0.2 MeV during the whole experiment, with 25 cGy at 0.6 MeV from 5 to 12 months, and with 50 cGy at 0.6 MeV from 5 to 13.5 months, whereas with 25 cGy they were decreased from 8 to 13.5 months as compared with control values (Table VI).

At autopsy, body weights of male F_1 mice of the 0.2 MeV energy level groups were not significantly altered (Table VII). Testis weights with 100 cGy were significantly lower than the non-irradiated group whereas adrenals were heavier. Relative testis weights (organ weight/body weight x1000) with 50 and 100 cGy were also significantly decreased as compared with the non-irradiated group and again adrenal values were increased (Table VIII).

Table VI. Body weights of F_1 female mice.

Group	3 months	4 months	5 months	6 months	7 months	8 months	9 months	10 months	11 months	12 months	13 months	14.5 months
0 cGy	24.2±1.4	26.0±1.9	27.0±3.2	29.6±3.5	32.0±4.4	34.2±5.1	36.2±5.8	37.6±6.2	40.8±6.0	42.8±6.0	43.6±6.1	43.1±6.4
0.2 MeV												
12.5 cGy	24.7±2.0	26.0±2.3	27.9±2.9	30.2±3.3	31.1±3.6	33.9±4.3	35.8±4.4	38.0±5.1	41.1±6.2	41.9±6.8	42.8±7.2	42.8±7.1
25 cGy	24.1±1.5	25.4±2.1	27.1±2.9	28.3±2.7	30.0±2.8	30.7±3.1[b]	32.7±3.6[b]	33.6±3.7[b]	36.5±4.2[b]	37.9±4.4[a]	37.6±4.7[a]	38.3±4.6[b]
50 cGy	26.0±2.1[b]	28.6±4.2[a]	30.0±3.6[a]	32.6±4.4[b]	34.3±5.2	36.4±5.8	38.2±5.4	40.3±6.7	43.7±6.0	46.2±5.8	47.1±5.6	44.4±9.3
100 cGy	27.8±3.0[a]	31.0±3.2[a]	33.9±3.9[a]	36.6±3.3[a]	38.5±5.2[a]	40.3±4.2[a]	42.3±4.1[a]	44.0±3.4[a]	47.4±3.7[a]	49.9±2.8[a]	50.0±3.0[b]	48.9±3.5[b]
0.6 MeV												
12.5 cGy	24.5±1.8	25.8±3.2	28.4±3.6	29.7±4.2	31.5±4.3	35.1±6.1	38.3±6.3	38.3±6.7	40.7±6.9	41.0±6.7	40.7±6.9	39.6±6.9
25 cGy	24.6±2.3	27.1±2.9	31.3±4.9[a]	33.2±5.2[a]	35.4±5.2[a]	38.4±6.0[a]	40.9±6.0[a]	42.3±6.1[a]	45.3±6.3[a]	46.4±6.2[b]	45.8±10.9	47.4±6.6
50 cGy	24.7±1.3	27.7±2.4	32.3±3.4[a]	35.2±3.4[a]	38.9±3.2[a]	41.4±4.8[a]	44.6±4.5[a]	44.9±4.9[a]	48.8±6.2[a]	49.2±5.3[a]	49.8±5.2[b]	48.6±5.9[b]
100 cGy	26.5±2.5[b]	24.8±11.4	31.9±6.0[a]	34.0±7.1[b]	35.7±7.4	38.0±7.4	40.0±8.4	42.2±8.8	45.7±9.0	46.0±8.1	47.3±9.9	46.3±9.1

(Mean ± SD). [a]Significantly different from 0 cGy value (P<0.01). [b]Significantly different from 0 cGy value (P<0.05).

Table VII. Body and organ weight for F_1 male.

Group	Body weight	Liver	Kidney	Testis	Adrenal	Spleen
0 cGy	46.0±3.4	2.15±0.36	0.61±0.07	0.21±0.01	0.007±0.002	0.11±0.03
0.2 MeV						
12.5 cGy	45.1±3.8	2.20±0.33	0.62±0.07	0.20±0.02	0.006±0.001	0.10±0.03
25 cGy	44.5±4.1	2.05±0.28	0.59±0.08	0.20±0.03	0.006±0.001	0.10±0.02
50 cGy	47.6±3.2	2.30±0.36	0.63±0.09	0.20±0.002	0.007±0.002	0.12±0.06
100 cGy	45.2±2.2	2.19±0.38	0.58±0.04	0.18±0.05[b]	0.026±0.042[a]	0.13±0.12
0.6 MeV						
12.5 cGy	45.0±3.8	2.00±0.24	0.62±0.09	0.21±0.01	0.007±0.002	0.10±0.01
25 cGy	48.1±4.0	2.52±0.58	0.69±0.07[a]	0.21±0.02	0.009±0.002	0.12±0.05
50 cGy	47.8±3.4	2.27±0.38	0.61±0.05	0.19±0.05[b]	0.008±0.001	0.12±0.03
100 cGy	45.3±5.6	2.22±0.63	0.57±0.12	0.18±0.03[b]	0.008±0.003	0.11±0.03

(Mean ± SD). [a]Significantly different from 0 cGy value (P<0.01). [b]Significantly different from 0 cGy value (P<0.05).

Body and kidney weights with 25 cGy at the 0.6 MeV energy level were increased, along with the relative liver and kidney weights in 25 cGy were heavier than non-irradiated group but testis in 50 cGy was decreased.

Table IX summarizes data for tumors in male F_1 offspring. Most lesions were liver tumors. Incidences overall were 25.7, 8.3 4.8, 25.0 and 42.9% with 0, 12.5, 25, 50 and 100 cGy at the 0.2 MeV energy level, respectively, and 0, 37.5, 45.5 and 25% at 0.6 MeV. Incidences of liver tumors were 18.9, 8.3, 4.8, 25.0 and 28.6 % at the 0.2 MeV energy level, respectively, and 0, 31.3, 40.1 (P=0.03) and 25% at 0.6 MeV. Sizes and number of liver tumors did not significantly differ among the groups.

Female mouse body and organ weights are shown in Table X. Body weights with 25 cGy at 0.2 MeV were significantly decreased as compared with the non-irradiated group, and ovary and adrenal weights were significantly increased with 100 cGy and liver and kidney weights with 25 and 50 cGy. Relative adrenal weights with 12.5 cGy and liver with 100 cGy were significantly decreased whereas ovary values were elevated at 100 cGy (Table XI).

Regarding incidences of tumors in females, three tumors (4.7%, hemangioma, lymphoma and ovary) appeared in the non-irradiated group, and values were 3/23 (13%, hepatoma, lung and ovary tumors), 3/22 (14%, ovary tumor), 1/20 (5%, ovary tumor) and 0 in the 12.5, 25, 50 and 100 cGy groups at

Table VIII. Relative organ weight for F_1 male mice.

Group	Liver	Kidney	Testis	Adrenal	Spleen
0 cGy	46.7±7.2	13.3±1.1	4.5±0.3	0.16±0.04	2.5±0.7
0.2 MeV					
12.5 cGy	48.8±6.1	13.8±0.9	4.3±0.4	0.14±0.03	2.2±0.6
25 cGy	46.1±3.2	13.3±1.4	4.5±0.6	0.14±0.03	2.3±0.4
50 cGy	48.3±5.8	13.3±1.4	4.1±0.8[b]	0.15±0.03	2.5±1.3
100 cGy	48.5±7.8	12.8±1.1	3.9±1.0[b]	0.59±0.93[a]	3.2±3.0
0.6 MeV					
12.5 cGy	44.3±2.4	13.7±1.7	4.6±0.4	0.17±0.05	2.2±0.3
25 cGy	52.0±9.6[b]	14.5±0.9[a]	4.3±0.4	0.18±0.05	2.5±1.1
50 cGy	47.2±5.7	12.9±0.9	4.0±1.1[a]	0.17±0.03	2.5±0.5
100 cGy	48.2±9.1	12.6±1.4	4.1±0.7	0.17±0.05	2.4±0.5

(Mean ± SD). [a]Significantly different from 0 cGy value ($P<0.01$). [b]Significantly different from 0 cGy value ($P<0.05$).

Table IX. Incidence of tumors for F_1 male mice.

Group	Effective no. of animal	Tumor bearing animal	Incidence	Liver tumor size	No. of liver tumor per mouse	Other tumor
0 cGy	74	19 (25.7)	14 (18.9)	1.59±4.13	0.20±0.40	Lung papilloma
0.2 MeV						
12.5 cGy	24	2 (8.3)	2 (8.3)	1.04±3.53	0.08±0.28	
25 cGy	21	1 (4.8)	1 (4.8)	0.24±1.09	0.05±0.22	
50 cGy	20	5 (25.0)	5 (25.0)	1.57±3.45	0.35±0.67	
100 cGy	7	3 (42.9)	2 (28.6)	2.13±4.16	0.57±0.79	Hemangioma
0.6 MeV						
12.5 cGy	10	0	0	0	0	
25 cGy	16	6 (37.5)	5 (31.3)	4.18±7.03	0.38±0.62	Harderian
50 cGy	22	10 (45.5), P=0.08	9 (40.1)[a], P=0.03	1.23±2.19	0.59±0.85	Hemangioma
100 cGy	8	2 (25)	2 (25)	2.33±4.69	0.38±0.74	

(Mean ± SD).

the 0.2 MeV energy level, respectively. The figures were 0, 5/22 (22.7), 5/20 (25%, ovary tumor) and 1/9 (11.1%, ovary) at the 0.6 MeV energy level (Table XII).

Discussion

The present experiments showed clear increase in the incidence of abnormal sperm in C3H males following monoenergetic neutron irradiation, resulting in increased embryo lethality of F_1 offspring and liver tumors in surviving F_1 males. While the sperm abnormalities were energy dose-dependent, this did not appear to be the case for embryonic death and tumor incidence.

This lack of dose-dependence is in line with the literature. Inverse dose-dependence for fission spectrum neutron induction of somatic hprt deficiency mutations has been reported by Nakamura and Sawada (20) with mouse leukemia L5178Y cells and ^{252}Cf-fission neutrons. Brenner and Hall published an inverse dose effect model for neoplastic transformation *in vitro* following high LET irradiation (21). Furthermore, Zhang *et al* (17) reported different doses of neutrons to produce approximately linear changes in the frequency of micronuclei in root-tip cells of *Allium cepaonion* irradiated as either dry dormant seeds or seedlings. Balcer-Kubiczek *et al* (22) earlier found modification of fission neutron dose-response curves on varying the dose rate to be negligible or

Table X. Body and organ weight for F_1 female mice.

Group	Body weight	Liver	Kidney	Ovary	Uterus	Adrenal	Spleen
0 cGy	43.1±6.4	1.60±0.28	0.36±0.03	0.026±0.023	0.478±0.541	0.026±0.023	0.110±0.022
0.2 MeV							
12.5 cGy	42.8±7.1	1.63±0.22	0.37±0.04	0.022±0.005	0.378±0.124	0.022±0.005	0.108±0.024
25 cGy	38.3±4.6[b]	1.46±0.17	0.36±0.04	0.026±0.005	0.580±0.472	0.026±0.006	0.110±0.030
50 cGy	44.4±9.3	1.62±0.37	0.38±0.04	0.026±0.007	0.509±0.176	0.026±0.007	0.120±0.054
100 cGy	48.9±3.5[b]	1.62±0.23	0.40±0.05	0.070±0.138[a]	0.299±0.160	0.070±0.138[a]	0.129±0.052
0.6 MeV							
12.5 cGy	39.6±6.9	1.58±0.30	0.38±0.05	0.029±0.010	0.662±0.509	0.028±0.009	0.119±0.039
25 cGy	47.4±6.6	1.77±0.30[b]	0.40±0.06[a]	0.033±0.033	0.488±0.479	0.033±0.033	0.122±0.029
50 cGy	48.6±5.9[b]	1.95±0.33[a]	0.44±0.04[a]	0.021±0.006	0.742±0.828	0.021±0.006	0.120±0.023
100 cGy	46.3±9.1	1.69±0.48	0.37±0.08	0.058±0.088	0.256±0.171	0.058±0.088	0.103±0.042

(Mean ± SD). [a]Significantly different from 0 cGy value ($P<0.01$); [b]Significantly different from 0 cGy value ($P<0.05$).

Table XI. Relative body weight for F_1 female.

Group	Liver	Kidney	Ovary	Uterus	Adrenal	Spleen
0 cGy	37.3±5.4	8.59±1.22	0.606±0.495	11.85±17.04	0.237±0.186	2.85±1.02
0.2 MeV						
12.5 cGy	38.4±4.6	8.88±1.09[b]	0.525±0.168	9.16±3.75	0.205±0.057[b]	2.60±0.88
25 cGy	38.4±3.7	9.43±1.15	0.683±0.208	15.47±12.24	0.390±0.576	2.88±0.77
50 cGy	35.0±6.4	8.23±0.68	0.553±0.152	11.17±4.02	0.202±0.054	2.56±0.86
100 cGy	33.1±3.0[b]	8.15±0.90	1.375±2.649[b]	6.08±3.13	0.197±0.050	2.61±0.95
0.6 MeV						
12.5 cGy	40.1±4.5	9.74±1.45[a]	0.727±0.234	18.35±17.00	0.267±0.078	3.06±0.95
25 cGy	37.6±3.7	8.52±1.41	0.721±0.734	10.71±10.57	0.235±0.072	2.62±0.71
50 cGy	40.1±3.4	9.06±0.73	0.445±0.134	16.58±20.65	0.171±0.027	2.47±0.36
100 cGy	36.4±5.3	8.05±0.59	1.188±1.756	5.33±3.39	0.192±0.055	2.23±0.65

(Mean ± SD). [a]Significantly different from 0 cGy value ($P<0.01$). [b]Significantly different from 0 cGy value ($P<0.05$).

absent. On the other hand, Hill and Williams-Hill (23) observed that reduction of the dose rate of fission neutrons increases their effectiveness for transformation of C3H 10T1/2 cells. Watanabe *et al* (24) reported that a single ^{252}Cf neutron dose resulted in higher incidences of ovarian and Harderian gland tumors than the same total dose given at a low dose rate with B6C3F1 mouse whole body irradiation. Clearly there may be differences between the *in vitro* and *in vivo* situations. It is considered that cells with large chromosomal aberrations or other abnormalities might be able to survive *in vitro*, but *in vivo* they might not, so smaller non-lethal chromosomal changes such as point mutations, frame shifts, as small additions or deletions could be essential for tumor induction *in vivo*. The source of irradiation, strain, sex, age and plants or animals are all clearly factors which need to be taken into account when determining radiation sensitivity. Recently, we reported that there were no significant differences in the tumor induction rate among the different energy such as 0.18, 0.32, 0.6 and 1.0 MeV monoenergetic neutron irradiation (18). Sasaki *et al* (25) also mentioned that induction of chromosome aberrations is not clearly dependent on neutron energy. In conclusion, there have been no consistent differences in tumor incidence among the various energies of neutron irradiation applied.

Goud *et al* (26) reported that exposure of mice to ^{252}Cf neutrons and gamma rays resulted in a decrease in testis weight and a concomitant increase in frequency of abnormal sperm. According to Hugenholtz and Bruce (19) X-ray-

Table XII. Incidence of tumor for F_1 female mice.

Group	Effective no. of animal	Positive (%)	Type of tumor
0 cGy	64	3 (4.7)	Hemangioma, lymphoma, ovary
0.2 MeV			
12.5 cGy	23	3 (13.0)	Hepatoma, lung, ovary
25 cGy	22	3 (13.6)	Ovary 3
50 cGy	20	1 (5.0)	Ovary
100 cGy	9	0	
0.6 MeV			
12.5 cGy	19	0	
25 cGy	22	5 (22.7)	Hepatoma, lymphoma, ovary 2, sarcoma
50 cGy	20	5 (25.0)	Ovary 5
100 cGy	9	1 (11.1)	Ovary

induced abnormalities in sperm are transmissible up to the F_2 generation as dominant mutations. Nomura (27,28) demonstrated an increase in the dominant lethality and congenital malformations in offspring of male or female mice irradiated with X-rays (6) or treated with urethane (27,28). These findings were further confirmed by Kirk and Lyon (29), West *et al* (30) and Lyon and Renshaw (31), using the same dose but different strains of mice. Nomura (6) also reported increased fetal death of F_1 offspring after paternal irradiation at the stage of spermatozoa and spermatids in a dose-dependent manner. Kurishita *et al* (32) demonstrated that external abnormalities are induced in offspring of male mice following treatment of germ cells at the spermatogonia stage with ^{252}Cf neutrons and the dose-response curve was linear up to 0.95 cGy. Streffer (33) similarly observed that a transgenerational transmission occurs for ionizing radiation-induced congenital malformations as well as for genomic instability, the latter measured at the chromosome level. Carls *et al* (34) described that ionizing radiation exposure of the germline can induce delayed DNA deletions in offspring mice. They suggested that DNA deletion events are implicated in the onset of carcinogenesis and a similar phenomenon in humans may account for a portion of childhood cancers. Nomura (6) found the incidence of tumors in F_1 mice of the ICR strain to increased, in this case dose-dependently, after paternal exposure to 36, 216 or 364 cGy of X-rays at the stage of spermatozoa, spermatids or spermatogonia. Of the tumors occurring in the F_1 offspring, 90% were lung tumors. Daher *et al* (35) reported that paternal X-ray irradiation resulted in reduction of litter size and a marginally significant doubling of the leukemia/lymphoma rate in the offspring in N5 strain mice, over a 1 year observation period. Urethane treatment of F_1 offspring derived from irradiated parents caused a 2.4 times greater incidence of tumors than observed in untreated controls (36). Vorobtsova *et al* (37) reported similar results with a different mouse strain. Mewissen *et al* (38) found that repeated administration of ^3H_2O as the drinking water to C57BL/6M males before mating over several generations gave rise to hereditary adenocarcinomas in the small intestine. Essentially comparable effects of chemical carcinogens have been reported (39-41). A high incidence of liver tumors was observed in the F_1 offspring of C3H male mice which had been exposed to 50 cGy of ^{252}Cf neutrons and mated with C57BL/6 females (8,9). In the present experiment, similar results were observed with 50 cGy especially at the 0.6 MeV energy level. Shay *et al* (42) documented that when 35- to 46-day-old Wistar rat females were treated with 3-methylcholanthrene using gastric tubes every day for two months and then mated with untreated males, the incidence of cancer was increased significantly in F_1 and F_2 offspring. Tomatis *et al* (5) subsequently found in the BDV1 rat system that the incidence of nerve tumors was significantly elevated in the F_1 generation when mating occurred two weeks after treatment of 9-week-old male rats with 80 mg/kg of ethylnitrosourea. Dasenbrock *et al* (43) described that maternal preconceptual exposure in C57BL/6J mice to radiation is associated with a moderately increased incidence of liver and lung tumors in the male descendants. The incidence of total tumors in the F_1 offspring, however, was not different from the control value. Lord *et al* (44) reported that with methylnitrosourea following preconceptional paternal contamination with ^{239}plutonium the second generation excess of leukemia appears to be the result of preconceptional paternal irradiation and may be related to inherited changes that affect the development of haemopoietic stem cells. The evidence in humans is most derived from case reports and epidemiological studies of consequences to the progeny of paternal occupational exposure to chemicals, ionizing radiation and electromagnetic fields prior to conception (3,45-47). Dasenbrock *et al* (43) indicated that maternal preconceptual X-ray exposure to radiation is associated with a moderately increased incidence of liver and lung tumors in male descendants in C57BL/6N mice. Thus the fact that genetic damage to parental germ cells can be transmitted to the offspring as an origin of carcinogenesis has been well documented, and this was confirmed in the present experiment.

However, Cattanach *et al* (48) described no significant increase but seasonal changes in the incidence of lung tumors in offspring of BALB/cJ or C3H/Heh mice exposed to X-rays following the experimental protocol of Nomura (6). Evidence for such seasonal changes in tumor incidence has been published and this relates to experiments carried out in insufficiently controlled animal facilities and experimental conditions, e.g., animals exposed to outdoor light. In fact, change of the light-dark interval significantly influences tumor frequencies in mice (49). Cattanach *et al* (48) also reported that reduction in litter size in paternally irradiated groups might be evidence of genetic damage, i.e., dominant lethality, resulting from the radiation exposure.

As a general rule, heavier mice are more likely to develop spontaneous and induced tumors earlier and caloric restriction decreases body weights and tumor incidences and increases longevity. Selby *et al* (50) suggested that induced dominant lethality in mice or rats with increased tumor rates have no relation with induction of dominant tumor mutations. In the

present experiment numbers of offspring were lower with 100 cGy at both energy levels and the fact that only a few animals survived means that the incidence of liver tumors might not have been accurate. The range of gene damage is presumably very wide, given the sperm abnormalities and the embryo lethality and malformations, and many embryos died, so that surviving animals might have been those less susceptible to induction of tumors. However, if gene damage is limited, tumor-prone animals might survive, resulting in greater causation of tumors. Nomura suggested that germ-line exposure is a very early tumorigenesis by itself. It is possible that the lack of increase in lung tumors reported by Cattanach *et al* (48) may be attributable to increased incidence of embryo lethality caused by high doses of paternal X-ray irradiation.

In conclusion, the results of the present study indicate that paternal exposure to radiation is associated with an increased incidence of liver tumors in the male descendants. While our study was not designed to investigate the mechanism of transmission of increased risk, the results are in keeping with the hypothesis of a germ line-transmitted hereditary effect of monoenergetic neutron irradiation.

Acknowledgements

We are grateful to Professor T. Nomura, Osaka University, and to Dr M.A. Moore for critical reading of this manuscript, and Mr. T. Nishioka for technical assistance.

References

1. Napalkov NP, Rice JM, Tomatis L and Yamasaki H: Perinatal and multigeneration carcinogenesis. IARC Scientific Publication, Lyon, 96, 1989.
2. Tomatis L, Narod S and Yamasaki H: Transgeneration transmission of carcinogenic risk. Carcinogenesis 13: 145-151, 1992.
3. Tomatis L: Transgeneration carcinogenesis: a review of the experimental and epidemiological evidence. Jpn J Cancer Res 85: 443-454, 1994.
4. Gardner MJ, Snee MP, Hall AJ, Powell CA, Downes S and Terrell JD: Results of the case-control study of leukemia and lymphoma among young people near Sellafield nuclear plant in West Cumbria. Br Med J 300: 423-429, 1990.
5. Tomatis L, Cabral JRP, Likhachev AJ and Ponomrkov V: Increased cancer incidence in the progeny of male rats exposed to ethylnitrosourea before mating. Int J Cancer 28: 475-478, 1981.
6. Nomura T: Parental exposure to X rays and chemicals induces heritable tumors and anomalies in mice. Nature 296: 575-577, 1982.
7. Takahashi T, Watanabe H, Dohi K and Ito A: ^{252}Cf relative biological effectiveness and inheritable effect of fission neutrons in mouse liver tumorigenesis. Cancer Res 52: 1948-1953, 1992.
8. Watanabe H, Takahashi T, Lee JY, *et al*: Influence of paternal ^{252}Cf neutron exposure on abnormal sperm, embryonal lethality, and liver tumorigenesis in the F1 offspring of mice. Jpn J Cancer Res 87: 51-57, 1996.
9. Shoji S, Masaoka Y, Kurosumi M, Katoh O and Watanabe H: Tumorigenesis in F_1 offspring mice following paternal 12.5 cGy ^{252}Cf fission neutron irradiation. Oncol Rep 5: 1175-1178, 1998.
10. Miller RC, Marino SA, Martin SG, *et al*: Neutron-energy-dependent cell survival and oncogenic transformation. J Radiat Res (Tokyo) (Suppl) 40: 53-59, 1999.
11. Pandita TK and Geard CR: Chromosome aberrations in human fibroblasts induced by monoenergetic neutrons. I. Relative biological effectiveness. Radiat Res 145: 730-739, 1996.
12. Kubota N, Okada S, Nagatomo S, *et al*: Mutation induction and RBE of low energy neutrons in V79 cells. J Radiat Res (Tokyo) (Suppl) 40: 21-27, 1999.
13. Tanaka K, Gajendiran N, Endo S, Komatsu K, Hoshi M and Kamada N: Neutron energy-dependent initial DNA damage and chromosomal exchange. J Radiat Res (Tokyo) (Suppl) 40: 36-44, 1999.
14. Tanaka K, Kobayashi T, Sakurai Y, Nakagawa Y, Endo S, Hoshi M: Dose distributions in a human head phantom for neutron capture therapy using moderated neutrons from the 2.5 MeV proton-^{7}Li reaction or from fission of ^{235}U. Phys Med Biol 46: 2681-2695, 2001.
15. Gajendiran N, Tanaka K and Kamada N: Comet assay to sense neutron 'fingerprint'. Mutat Res 452: 179-187, 2000.
16. Schmid E, Schlegel D, Guldbakke S, Kapsch RP and Regulla D: RBE of nearly monoenergetic neutrons at energies of 36 keV-14.6 MeV for induction of dicentrics in human lymphocytes. Radiat Environ Biophys 42: 87-94, 2003.
17. Zhang W, Fujikawa K, Endo S, Ishikawa M, Ohtaki M, Ikeda H and Hoshi M: Energy-dependent RBE of neutrons to induce micronuclei in root-tip cells of *Allium cepa* onion irradiated as dry dormant seeds and seedlings. J Radiat Res (Tokyo) 44: 171-177, 2003.
18. Watanabe H, Kashimoto N, Kajimura J, Ishikawa M and Kamiya K: Tumor induction by monoenergetic neutrons in B6C3F1 mice. J Radiat Res (Tokyo) 48: 205-210, 2007.
19. Hugenholtz AP and Bruce WR: Radiation induction of mutations affecting sperm morphology in mice. Mutat Res 107: 177-185, 1983.
20. Nakamura N and Sawada S: Reversed dose-rate effect of RBE of ^{252}calfornium radiation in the induction of 6-thioguanine-resistant mutations in mouse L5176Y cells. Mutat Res 201: 65-71, 1988.
21. Brenner DJ and Hall EJ: The inverse dose-rate effect for oncogenic transformation by neutrons and charged particles: a plausible interpretation consistent with published data. J Radiat Biol 58: 745-758, 1990.
22. Balcer-Kubiczek EK, Harrison GH, Hill CK and Blakely WF: Effects of WR-1065 and WR-151326 on survival and neoplastic transformation in C3H/10T1/2 cells exposed to TRIGA or JANUS fission neutrons. Int J Radiat Biol 63: 37-46, 1993.
23. Hill CK and Williams-Hill D: Neutron carcinogenesis: past, present and future. J Radiat Res (Tokyo) (Suppl) 40: 117-127, 1999.
24. Watanabe H, Okamoto T, Yamada K, *et al*: Effects of dose rate and energy level on fission neutron (^{252}Cf) tumorigenesis in B6C3F1 mice. J Radiat Res (Tokyo) 34: 235-239, 1993.
25. Sasaki MS, Endo S, Ejima Y, *et al*: Effective dose of A-bomb radiation in Hiroshima and Nagasaki as assessed by chromosomal effectiveness of spectrum energy photons and neutrons. Radiat Environ Biophys 45: 79-91, 2006.
26. Goud SN, Feola JM and Maruyama Y: Sperm shape abnormalities in mice exposed to californium-252 radiation. Int J Radiat Biol 52: 755-760, 1987.
27. Nomura T: Transmission of tumors and malformations to the next generation of mice subsequent to urethan treatment. Cancer Res 35: 264-266, 1975.
28. Nomura T: Transgenerational effects from exposure to environmental toxic substances. Mutat Res 659: 185-193, 2008.
29. Kirk M and Lyon MF: Induction of congenital malformations in the offspring of male mice treated with X-rays at pre-meitic and post-meiotic stages. Mutat Res 125: 75-85, 1984.
30. West JD, Kirk Y, Goyder Y and Lyon MF: Discrimination between the effects of X-ray irradiation of the mouse oocyte and uterus on the induction of dominant lethals and congenital anomalies. I. Embryo-transfer experiments. Mutat Res 149: 221-230, 1985.
31. Lyon MF and Renshaw R: Induction of congenital malformations in mice by parental irradiation: transmission to later generations. Mutat Res 198: 277-283, 1988.
32. Kurishita A, Ono T, Okada S, Mori Y and Sawada S: Induction of external abnormalities in offspring of male mice irradiated with ^{252}Cf neutron. Mutat Res 268: 323-328, 1992.
33. Streffer C: Transgenerational transmission of radiation damage: genomic instability and congenital malformation. J Radiat Res (Tokyo) (Suppl B) 47: B19-B24, 2006.
34. Carls Nand Schiestl RH: Effect of ionizing radiation on transgenerational appearance of p(un) reversions in mice. Carcinogenesis 20: 2351-2354, 1999.
35. Daher A, Varin M, Lamontagne Y and Oth D: Effect of preconceptional external or internal irradiation of N5 male mice and the risk of leukemia in their offspring. Carcinogenesis 19: 1553-1558, 1998.

36. Nomura T: X-ray-induced germ-line mutation leading to tumors. Its manifestation in mice given urethane post-natally. Mutat Res 121: 59-65, 1983.
37. Vorobtsova IE and Kitaev EM: Urethane-induced lung adenomas in the first-generation progeny of irradiated male mice. Carcinogenesis 11: 1931-1934, 1988.
38. Mewissen J, Ugarte AS and Rust JH: Tumeur intestinale hereditaire observé après irradiation de generations multiples d'une lignee germinale male de la souris C57BL/6. CR Soc Biol 178: 230-235, 1984.
39. Strong LC: Genetic analysis of the induction of tumors by methylcholanthrene. Am J Cancer Inst 39: 347-349, 1940.
40. Strong LC: Genetic analysis of the induction of tumors by methylcholanthrene. IX. Induced and spontaneous adenocarcinomas of the stomach in mice. J Natl Cancer Inst 5: 339-362, 1940.
41. Boutwell RK: Some biological aspects of skin carcinogenesis. Prog Exp Tumor Res 4: 207-250, 1964.
42. Shay H, Gruenstein M and Weinberger M: Tumor incidence in F_1 and F_2 generations derived from female rats fed methylcholanthrene by stomach tube prior to conception. Cancer Res 12: 296, 1952.
43. Dasenbrock C, Tillmann T, Ernst H, *et al*: Maternal effects and cancer risk in the progeny of mice exposed to X-rays before conception. Exp Toxicol Path 56: 351-360, 2005.
44. Lord BI, Woolford LB, Wang L, *et al*: Induction of lymphohaemopoietic malignancy: impact of preconception paternal irradiation. Int J Radiat Biol 74: 721-728, 1998.
45. Savitz DA and Chen JH: Parental occupation and childhood cancer: review of epidemiologic studies. Env Health Per 88: 325-337, 1990.
46. O'Leary LM, Hicks AM, Peters JM and London S: Parental occupational exposures and risk of childhood cancer: a review. Am J Ind Med 20: 17-35, 1991.
47. Pearce MS, Hammal DM, Dorak MT, McNally RJ and Parker L: Paternal occupational exposure to electro-magnetic fields as a risk factor for cancer in children and young adults: a case-control study from the North of England. Ped Blood Cancer 49: 280-286, 2007.
48. Cattanach BM, Patrick G, Papworth D, *et al*: Investigation of lung tumour induction in BALB/cJ mice following paternal X-irradiation. Int J Radiat Biol 67: 607-615, 1995.
49. Nakajima H, Narama I, Matsuura T and Nomura T: Enhancement of tumor growth under short light/dark cycle in mouse lung. Cancer Lett 78: 127-131, 1994.
50. Selby PB, Earhart VS and Raymer GD: The influence of dominant lethal mutations on litter size and body weight and the consequent impact on transgenerational carcinogenesis. Mutat Res 578: 382-394, 2005.